CORRECTION FOR DISTORTIONS OF MAGNETOTELLURIC FIELDS: LIMITS OF VALIDITY OF THE STATIC APPROACH

B. SH. SINGER

The Institute of the Physics of the Earth, US Academy of Sciences Troitsk, Moscow Region 142092, Russia

(Received 21 October 1990; accepted 14 August 1991)

Abstract. Subsurface inhomogeneities can be classified in three categories depending on the comparison of their sizes against the effective skin depth and "adjustment distance". These categories are geological noise, local and regional inhomogeneities.

Due to its random nature, geological noise leads to uncontrollable distortions of the magnetotelluric field. Such methods as curve shifting, distortion tensor techniques, decomposition and spatial filtering can effectively be used to correct for static shift caused by geological noise.

It is shown that the effects of local and regional subsurface inhomogeneities reduce to static shifts of MT-curves when rather rigid conditions are satisfied. The methods used to suppress the effect of geological noise have limited applicability to local and regional inhomogeneities, which can be accurately accounted for only by modelling.

1. Introduction

Due to its importance for magnetotellurics, the problem of local distortions of electromagnetic fields has a rather long history. Local distortions reduce the quality and resolving power of MT-soundings and create erroneous interpretations. There exist a number of approaches to the problem but none completely addresses all aspects of distortion. Further development of data acquisition, processing and interpretation tools will be unlikely to solve the problem in itself. This means that some special measures will always be necessary to remove the distortions before the data can be interpreted correctly.

Inductive and galvanic distortions taking place in 2-D media were first described by Berdichevsky and Dmitriev (1976a, b). Inductive distortions result from the excessive currents flowing in areas adjacent to the observation point. As a result, MT sounding in the vertical direction is often influenced by lateral conductivity structure as well. The distortions usually affect the ascending branch of the apparent resistivity curve $\rho_a(T)$ and have negligible effect on the descending branch. Inductive distortion can introduce spurious inflections on the curve, leading to an erroneous impression that additional layers exist in the medium.

In 2-D media, the S-effect takes place for B-polarized fields observed over a surface inhomogeneity. It does not affect the ascending branch but vertically shifts the descending one. This leads to erroneous conclusions on depths of layers. Some distance from the anomaly the so called "edge effect" can be observed

Surveys in Geophysics **13**: 309–340, 1992.
© 1992 *Kluwer Academic Publishers. Printed in the Netherlands.*

(Berdichevsky and Dmitriev, 1976b). It spoils the ascending branch of the curve and shifts the descending one. The value of the effect depends upon the distance from the anomaly. In 3-D media more complicated effects, such as flowing around, current channeling, etc. take place. The name "three-dimensional S-effect" is sometimes used in such cases. Instructive examples of modelling 3-D effects can be found in (Vasseur and Weidelt, 1977), (Singer *et al.*, 1984) and (Park, 1985). As in 2-D media, the effect shifts that part of the $\rho_a(T)$ curve when inductive effects in the inhomogeneous layer become negligible. The apparent impedance phase is not affected.

The earth's surface roughness also is a source of MT field distortions (Dmitriev and Tavartkiladze, 1975). Topographic distortions are frequency dependent at short periods and have static character at long periods. Significant distortions can originate from moderate surface roughness. The slope of the surface is often more important than the amplitude (Reddig and Jiracek, 1984).

The physical essence of the static effect has been described repeatedly. Current $\mathbf{j}$ flowing through geoelectrical inhomogeneities creates electric charges whose density is $\mathbf{j} \cdot \nabla(\epsilon_0/\sigma)$, where $\epsilon_0 = 10^{-9}/36\pi$ F/m, and σ is the specific conductivity. While the magnetic field

$$\mathbf{H} = \nabla \times \mathbf{A} \tag{1}$$

depends only on the current distribution as

$$\mathbf{A}(\mathbf{r}) = \int_{\mathbb{R}^3} \frac{\mathbf{j}(\mathbf{r}')}{|\mathbf{r} - \mathbf{r}'|} \frac{\mathrm{d}v'}{4\pi}, \tag{2}$$

the electric field

$$\mathbf{E} = \iota\omega\mu_0\mathbf{A} - \nabla\Phi, \tag{3}$$

is sensitive to the charge distribution ($\mu_0 = 4\pi \cdot 10^{-7}$ H/m), as

$$\Phi(\mathbf{r}) = \int_{\mathbb{R}^3} \frac{\mathbf{j} \cdot \nabla(\epsilon_0/\sigma)}{|\mathbf{r} - \mathbf{r}'|} \frac{\mathrm{d}v'}{4\pi}. \tag{4}$$

To reveal geoelectrical structure at depth z, the frequency ω is chosen so that induced currents would flow at this depth. Although only a small part of the currents flow at the earth's surface, they can produce significant charge if inhomogeneities exist there. It follows from Equations (1)–(4) that the galvanic part of the electric field prevails at low frequencies, while the major part of the magnetic field emerges from the currents flowing at depth z. If the medium is laterally uniform at this depth, then both the secondary and total magnetic fields will be uniform and any further decrease in frequency will affect only their amplitudes. This means that the surface current distribution can be found from the DC-problem solution. Thus the spatial distribution and the phase shift of the electric field relative to the magnetic field will be conserved. This justifies the term "static distortions". We shall terminate here the discussion on the physical essence of static distortion. More detailed consideration can be found in the previous excellent review (Jiracek, 1990) and two earlier ones (Jones, 1983; Menvielle, 1988).

2. Methods to Correct for Surface Inhomogeneities

The field configuration is usually chosen to represent basic peculiarities of the electromagnetic field. Therefore the distance between the neighboring points of observation is, as a rule, smaller than the depth of sounding. The same is valid for a numerical modelling mesh. Inhomogeneities whose size is smaller than or comparable with the distance between nodes of the experimental or numerical mesh cannot be adequately represented on the mesh. They are small also in comparison with the skin depth and will be referred to below as "geological noise". Typical dimensions of such inhomogeneities do not usually exceed several kilometers. Inhomogeneities which are comparable with or greater than the skin depth but smaller than the "adjustment distance" will be referred to as "local inhomogeneities". For inhomogeneities whose dimensions are comparable with the "adjustment distance" the term "regional inhomogeneities" will be used.

Methods used to correct for subsurface inhomogeneity distortions such as curve shifting, distortion tensor techniques, decomposition, spatial filtration and modelling are discussed below. Some of them can be used as a remedy against both geological noise and local inhomogeneities, others have only limited usage. For example the geological noise effect on practical MT sounding cannot be modeled numerically.

In 2-D situation and in the frequency band of deep MTS, the effects of the subsurface inhomogeneities are often negligible in the E-polarized field, which can be interpreted using one dimensional inversion. Exceptions are to be made for deep conductive fractures or sea shore areas, when 2-D interpretation is unavoidable. Sometimes B-polarization is more informative (Wannamaker *et al.*, 1989). Local 2-D inhomogeneities can in both cases be incorporated in the model, but geological noise can not, as corresponding inhomogeneities are three-dimensional. The effects of geological noise should be taken into account for both E- and B-polarized fields.

Due to its uncontrollable character, geological noise leads to dangerous distortions of the MT field. Fortunately, the corresponding inhomogeneities are so small that even at high frequencies only a negligible part of the currents is induced in the inhomogeneities. In other words, the whole MT frequency band can be considered as the low frequency band with respect to geological noise. Thus, inductive distortions created by the geological noise inhomogeneities are negligible; the main effect is the static distortion of the electric field.

2.1. Curve shifting and distortion tensor techniques

Examples of how a small inhomogeneity affects the apparent resistivity curves are shown in Figure 1 (Sternberg *et al.*, 1988) and Figure 2 (Chouteau and Bouchard, 1988). The effect of geological noise on the apparent resistivity curves is manifested as a frequency-independent vertical shift. The shift value can be evaluated at each field point if there exists some additional information on the conductivity distribution just under the point.

The information can be acquired from the global conductivity distribution (Rokityansky, 1982). The global curve in Figure 3 was provided by Fainberg (1983a, b) as a result of careful data selection. Corrections of Sq-harmonic frequency responses were made to compensate the effect of the oceans and the sedimentary cover. The short period bound of the curve is at the period $T = 8h$, which corresponds to the depth 400 km. It was assumed that the conductivity distribution becomes laterally uniform at such depth, and hence any undistorted MT curve should coincide with the global one at periods $T > 8h$. This gives a key to selection of undistorted MT curves. The procedure can be used only if the MT curves have a sufficiently long low-frequency branch.

The MT curves in Figure 3 were obtained on the East European Platform and selected as undistorted (Vladimirov and Dmitriev, 1972). If one continues the global curve along the envelope of the MT curves, the normal curve of the East

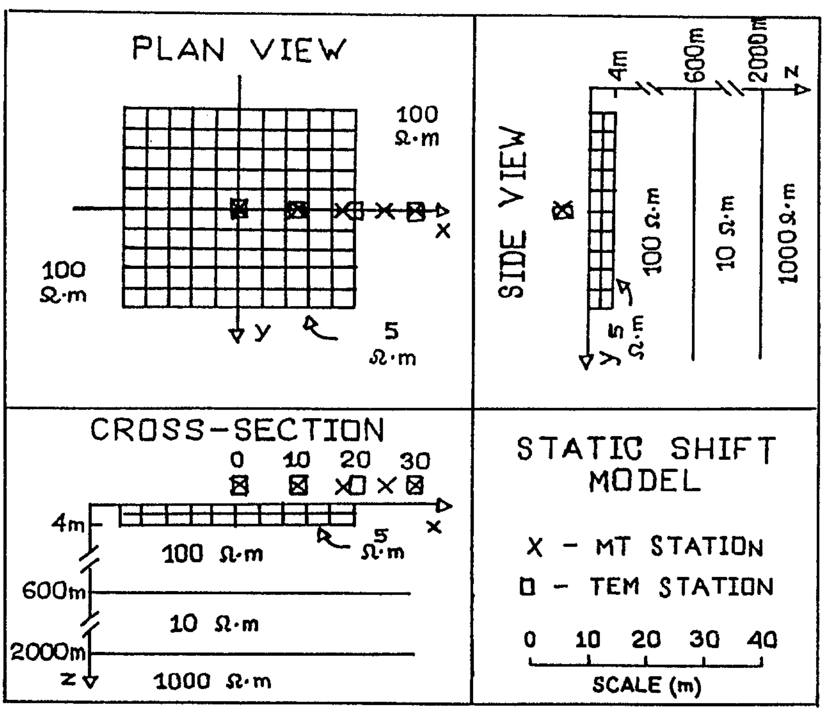

a

Fig. 1a.

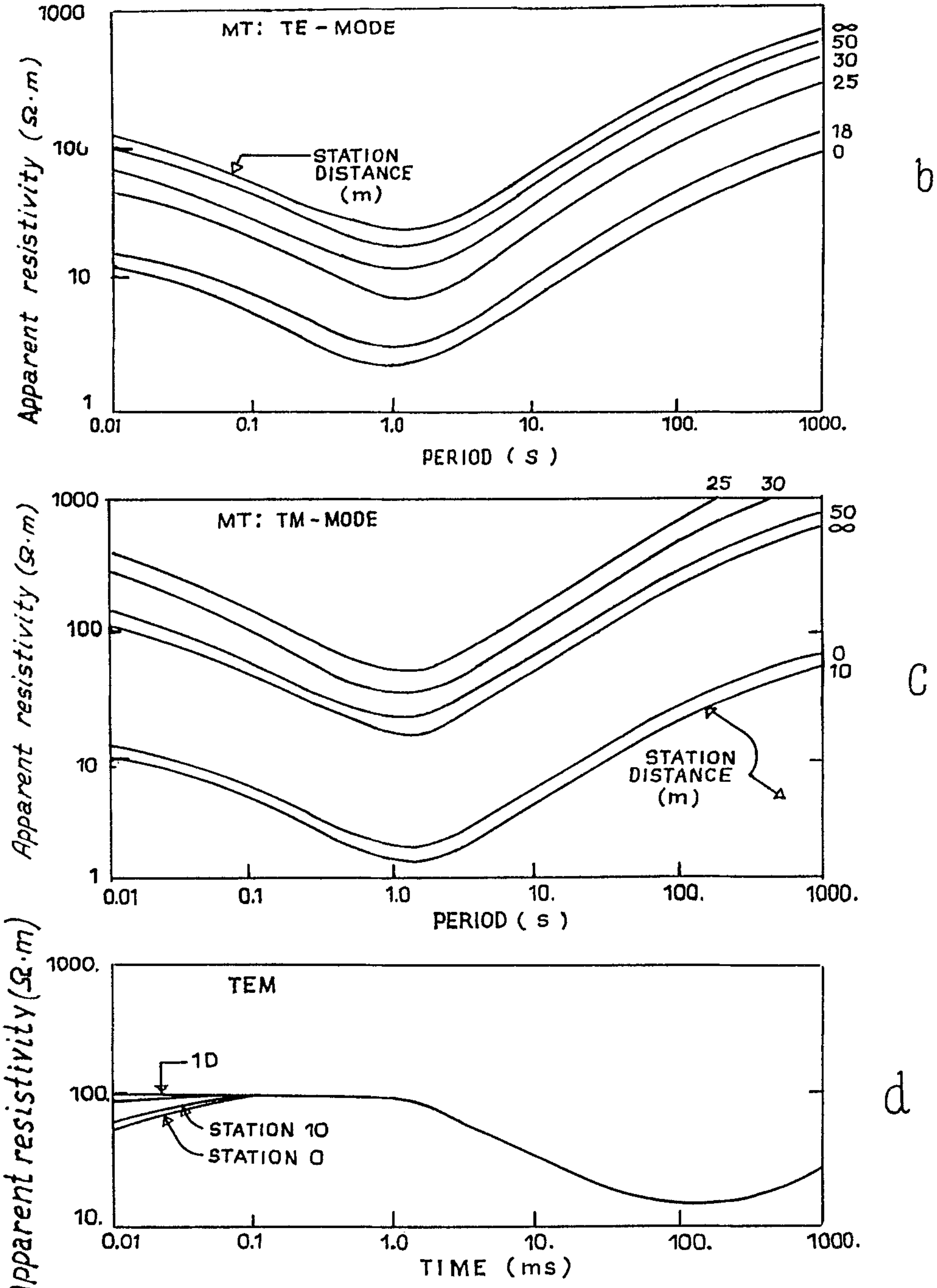

Fig. 1. Model example of the static shift effect (Sternberg *et al.*, 1988). (a) The model and the acquisition geometry, (b) MT apparent resistivity curves for TE-polarization. Station distance from the center of the anomaly is noted on a plot, (c) MT apparent resistivity curves for TM-polarization, (d) TEM apparent resistivity curves.

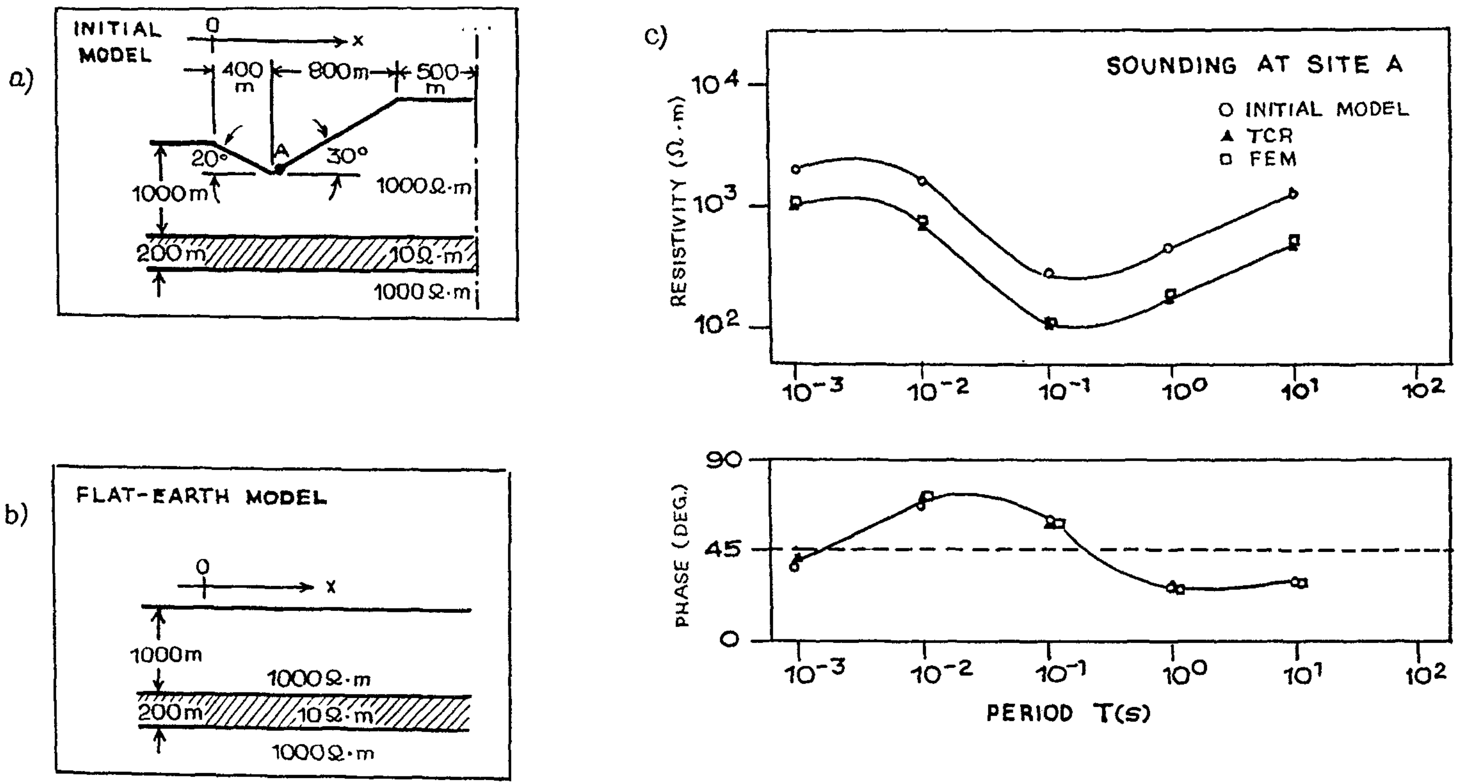

Fig. 2. Topographic distortion of MT curve and its stripping by distortion tensor technique (Chouteau and Bouchard, 1988). (a) Geometry of initial model with topography over layered earth. (b) Geometry of flat earth model. (c) Initial model, terrain corrected (TCR), and flat earth model (FEM) TM apparent resistivity and impedance phase sounding curves at site A in (a).

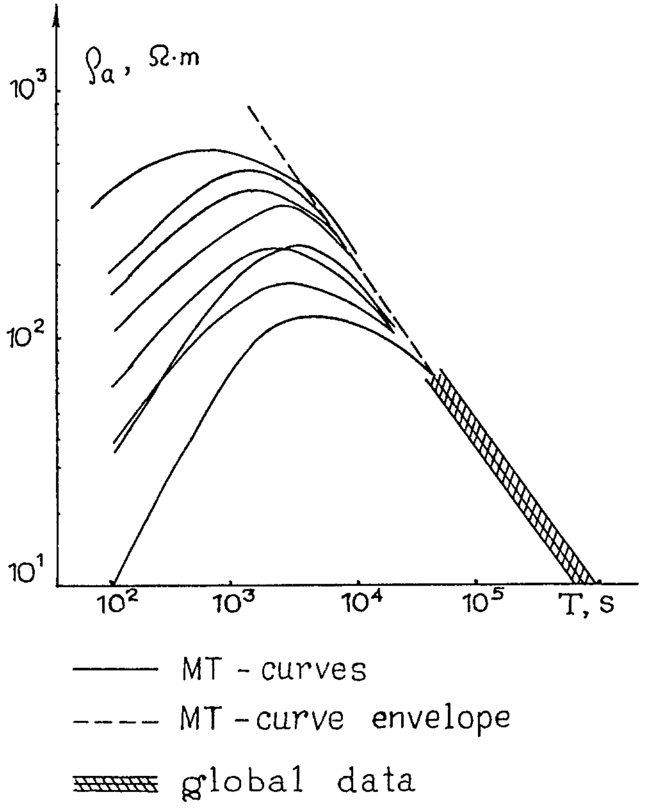

Fig. 3. The standard global curve (Fainberg, 1983a,b) together with undistorted MT-curves at East European Platform.

European Platform with the bound at $T = 1h$ is obtained (Fainberg, 1983a). The approach has been used in (Vanyan *et al.*, 1977; Vanyan *et al.*, 1980; Avagimov *et al.*, 1981; Berdichevsky *et al.*, 1989).

In a number of regions the descending branches of MT curves either undershoot or overshoot the global curve. If the subsurface conductivity distribution is known then numerial modelling is the most natural way to obtain the regional reference curve. The MT curve undistorted by geological noise should have the descending branch which coincides with the normal regional curve. When using this approach it should be kept in mind that deep inhomogeneities can shift the low frequency branch (Berdichevsky *et al.*, 1984) as well as a subsurface one.

An alternative approach was considered in (Berdichevsky *et al.*, 1988). It was proposed to shift individual MT curves to a position corresponding to some "averaged" value of the surface conductance. Additional information on the section can also be acquired if there exist a simple parameterization of the conductivity distribution in one of the layers (Jones, 1988). Independently of which of the layers has been referred to for the static shift correction procedure, the resultant curve contains adequate information on layers just below the inhomogeneous layer responsible for the shift down to the next inhomogeneous layer if the reference layer occupies the intermediate position.

It seems the most promising approach to a static shift correction is based on utilization of auxiliary magnetic field measurements. Unlike the telluric field the magnetic field is much less affected by surface inhomogeneities. Transient electromagnetic (TEM) sounding was used by Andrieux and Wightman (1984). TEM sounding curves for the model in Figure 1a are shown in Figure 1d (Sternberg *et al.*, 1988). It can be seen that at $t = 0.1$ ms, TEM curves become insensitive to the surface inhomogeneity. Thus the joint interpretation of MT and TEM curves is a way to abolish the static shift. Naturally such interpretation is possible only if the maximum depth of TEM sounding is greater than the minimum depth of MT sounding and the medium at this depth interval is laterally uniform. The logical approach to find a correct reference curve is to carry out the TEM curve inversion followed by MT curve calculation for the revealed structure (Pellerin and Hohmann, 1990). The procedure was investigated numerically for a model consisting of a deep 3-D target and geological noise (Figure 4a). Distorted, undistorted, and calculated reference curves are shown in Figure 4b. It is curious that ρ^a_{xy}, ρ^a_{yx} curves are so close at high frequencies that they could be erroneously accepted as undistorted. The method extracts the ρ^a_{xy} curve which is close to the locally longitudinal one, and provides little information on the correct position of the ρ^a_{yx} curve. Auxiliary sounding was also implied in Kaufman (1988) where the idea to use the ratio of apparent impedances $Z_a(\omega)/Z_a(\omega_0)$ instead of the impedance itself was discussed.

Natural magnetic fields can also be useful in the static correction procedure (Larsen, 1977). Joint interpretation of MT and magnetovariational soundings is also the essence of "Electrical Conductivity Reference Exploration (ECRE)" (Wolfgram and Scharberth, 1986).

The methods just described are designed to correct the apparent resistivity curves. Of even greater importance is restoring the telluric field itself. In 2-D media the undistorted E-polarized electric field can be found if one integrates the vertical magnetic field. In more complicated 3-D media the distortion tensor technique can be used (Schmucker, 1970; Larsen, 1977; Hempfling, 1977; Mozley, 1982; Berdichevsky and Zhdanov, 1984; Bahr, 1985; Junge, 1986; Junge, 1988; Jiracek *et al.*, 1989).

The electric field at an observation point can be expressed via the undistorted electric field $\mathbf{E}^U_\tau$ using the distortion tensor $\hat{D}$:

$$\mathbf{E}_\tau = \hat{D}\mathbf{E}^U_\tau.$$

A similar expression is valid for distorted and undistorted impedances. If the normal impedance is known at one frequency then using the experimental fields it is possible to find the distortion tensor $\hat{D}$. In a frequency band where distortions

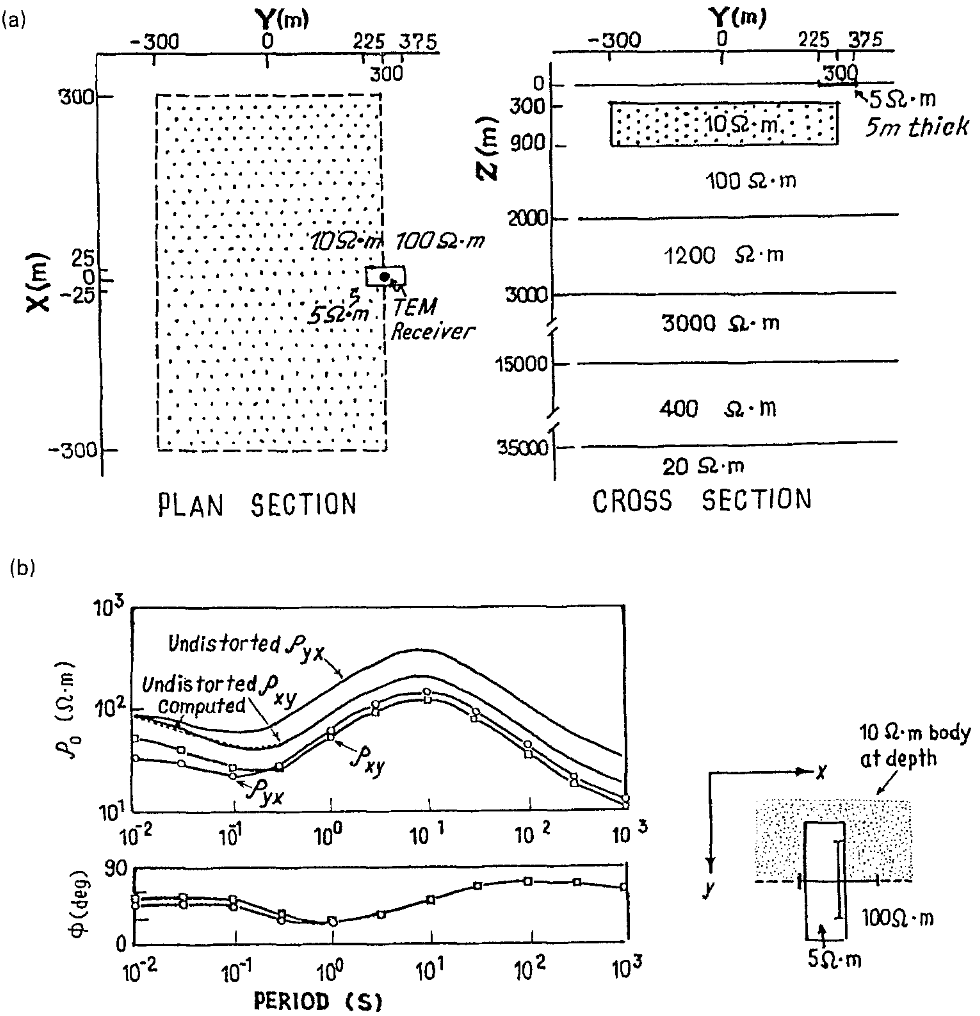

Fig. 4. Removal of surficial distortion in case of 3-D target object (Pellerin and Hohmann, 1990). (a) Geometry of 3-D 5 Ω · m, 5 m thick conductive surficial inhomogeneity and a large deeper 3-D 10 Ω · m body in a layered earth, central loop TEM receiver. (b) Synthetic ρ_{xy} amd ρ_{yx} together with undistorted and computed curves. 100 m crossed MT electrode array.

are static, the undistorted field can be found from $\hat{D}^{-1}\mathbf{E}_\tau$. Frequency dependent tensor stripping was discussed in (Chouteau and Bouchard, 1988; Jiracek *et al.*, 1989). The distortion tensor can also be modeled for local inhomogeneities, otherwise it should be determined on the basis of experimental data. It seems that the most consistent approach should use the field calculated for a model taking into account the local inhomogeneites as the undistorted field. The distortion tensor technique should then be invoked to strip the effect of geological noise.

It was shown in (Groom and Bailey, 1989) that if the regional structure is two dimensional and distorted by a 3-D inhomogeneity, then unique determination of the strike is possible. The main impedances are determined in this case up to some frequency independent factors.

2.2. Spatial filtering

Geological noise is a set of randomly distributed surface inhomogeneities whose deterministic separation is practically impossible. At the same time, geological noise causes enormous scatter in MT data. Apparent resistivity maps drawn for a single period look very irregular. Spatial filtering of such maps was used in (Berdichevsky and Nechaeva, 1975; Berdichevsky *et al.*, 1989). Another approach consists of averaging of apparent resistivity curves. Berdichevsky *et al.* (1980) classified the Baikal Region into 10 zones with conformal effective $\rho_a(T)$ curves. The curves belonging to each zone were averaged and only the averaged curve were used for the interpretation. Spatial curve averaging was used also in (Sternberg *et al.*, 1982; Warner *et al.*, 1983) and a number of other papers. Often it is the only tool available to correct for the distortions. Nevertheless, when using this approach one can never say with certainty that the averaged curve will not be shifted (Hermance, 1982).

A more consistent approach is based on the spatial filtration of the telluric field itself. This can be done in different ways. For example two smoothing procedures were proposed recently in (Kaufman, 1988). It should be noted also that a minimum level of intrinsic averaging is always involved in any MT experiment because of the finite length of electrical measurement dipoles. The observed magnetic field is measured at a point while the electric field is averaged along the dipole. If the dipole originates at $\mathbf{r}_1$ and terminates at $\mathbf{r}_2$, then the value measured is

$$(\mathbf{r}_2 - \mathbf{r}_1)\langle \mathbf{E}_\tau \rangle = \int_{\mathbf{r}_1}^{\mathbf{r}_2} \mathbf{E}_\tau(\mathbf{r})\, d\mathbf{r}.$$

This averaging provides an additional stabilization of the apparent impedance (Poll *et al.*, 1989; Jones, 1988).

The E-polarized field contains information not only on the medium at depth $0 < z \lesssim |\Lambda_0|$ just below the observation point (where $Z_0 = -\iota\omega\mu_0\Lambda_0$ is the impedance and $|\Lambda_0|$ is the skin depth) but on the lateral conductivity distribution at horizontal distances of order $|\Lambda_0|$. The same is true for the B-polarized field if the observed electric field is smoothed with a spatial window whose width is $|\Lambda_0|$ or greater. This is the basic concept of the "ElectroMagnetic Array Profiling (EMAP)" (Bostick, 1977; Bostick, 1984; Torres-Verdin, 1985; Word *et al.*, 1986). It was stressed in (Bostick, 1986) that if a profile is approximately orthogonal to strike the averaging effectively takes place along both directions. This statement is valid for quasi-two-dimensional structure. In three-dimensional media, the situation is more complicated as the electromagnetic field does not decompose into

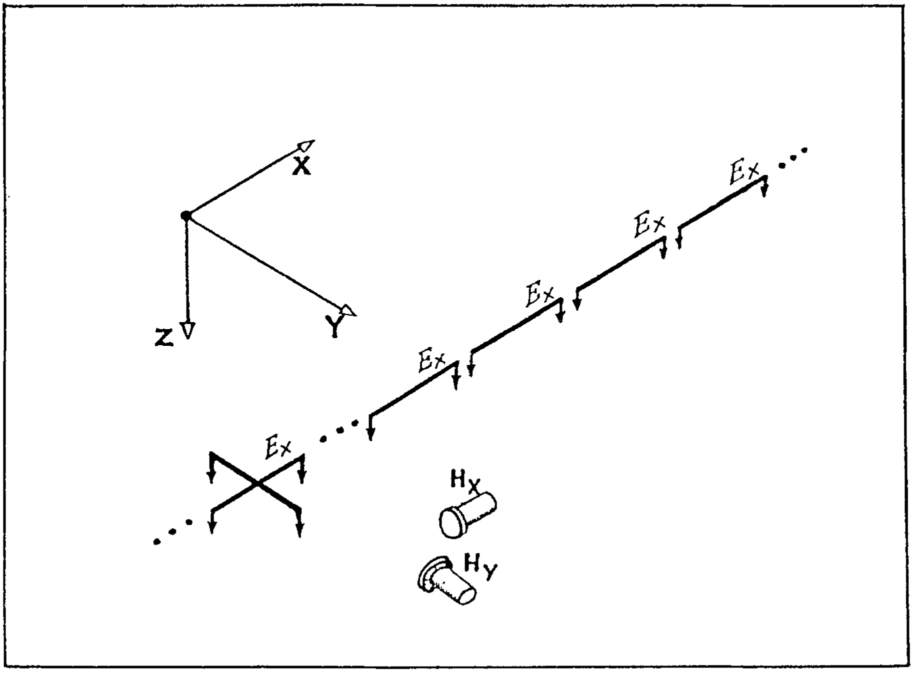

Fig. 5. The acquisition geometry for MT array survey of EMAP type (Shoemaker *et al.*, 1986). $\mathbf{E}_x$, $\mathbf{E}_y$ – electric dipoles, $\mathbf{H}_x$, $\mathbf{H}_y$ – magnetic field sensors.

E- and B-polarization modes. Hence only areal averaging would guarantee the necessary effect.

The typical EMAP sensor disposition is shown in Figure 5 (Shoemaker *et al.*, 1986). The dipole length is between 60 m and 600 m. At high frequencies when $|\Lambda_0|$ is smaller than the single dipole length, the signal is measured off every dipole. For lower frequencies, the weighted signals of several dipoles is combined. The window width ranges between $|\Lambda_0|$ and $3|\Lambda_0|$. It is not necessary to use very long electric arrays at low frequencies. Instead the transfer functions between the measured electric field and the magnetic field in a fixed reference point are calculated, and then the array can be moved to a new position. The important feature of EMAP is the employment of continuous arrays to avoid aliasing. Aliasing is practically unavoidable when sampling is used. The effective penetration depth is usually evaluated via the apparent impedance, which can be significantly scattered. Jones *et al.* (1989) proposed to use the electric field averaged along the profile to evaluate the cut off spatial frequency. The spatial averaging smooths out structures which are smaller than the skin depth. One dimensional inversion is usually used to interpret the EMAP acquired data. Some examples of 2-D interpretation also exist (Shoemaker *et al.*, 1986).

Spatial filtering as well as the other approaches designed to suppress the static

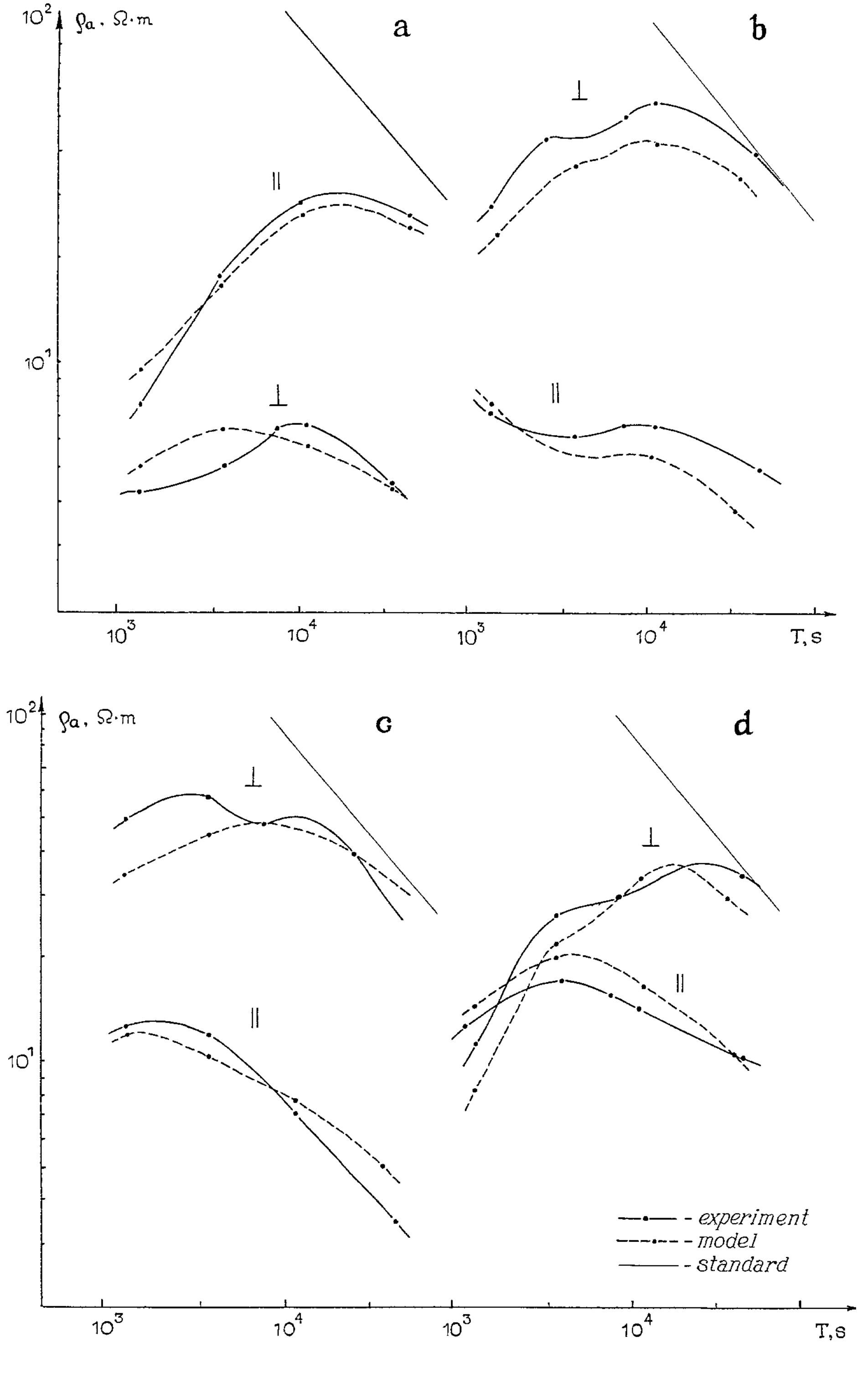

10^2
ρ_a, Ω·m
a
b
⊥
||
10^1
||
⊥
10^3
10^4
10^3
10^4
T, s
10^2
ρ_a, Ω·m
c
d
⊥
⊥
||
||
10^1
- experiment
- model
- standard
10^3
10^4
10^3
10^4
T, s

shift are first of all a remedy against geological noise. The same methods can be used in the case of local inhomogeneities, but information on the depths corresponding to the maximum of the $\rho_a(T)$ curve is lost in this case. Regional distortions can not be suppressed by spatial filtering.

2.3. Electromagnetic field modelling

The approach based on physical or numerical modelling has now become a practical tool for taking into account local and regional scale distortions. At the same time its application for geological noise in practical MT soundings is inhibited by insufficiency of experimental information, and limits on the performance of computers.

The modern state of physical modelling (Moroz *et al.*, 1975; Dosso *et al.*, 1989) makes it possible to simulate rather complicated earth models. There exists a large number of papers devoted to 3-D numerical modelling (Raiche, 1974; Weidelt, 1975; Hohmann, 1975; Ting and Hohmann, 1981; Hvozdara, 1981; Zhdanov and Spichak, 1980; Velikhov *et al.*, 1983; Park, 1985; Druskin and Knizhnerman, 1988; Wannamaker *et al.*, 1984; Vanyan *et al.*, 1984; Newmann, 1989).

A separate branch consists of thin sheet modelling programs (Vasseur and Weidelt, 1977; Singer *et al.*, 1984; Vanyan *et al.*, 1984; McKirdy *et al.*, 1985; Robertson, 1988). Thin sheet modelling programs appear to be an adequate tool to analyze and correct local and regional distortions as they make available sufficiently large numerical meshes on moderate performance computers. Thin sheet modelling was used for interpretation of MT observations in the Carpatian Region (Zhdanov *et al.*, 1987), the Ural Region (Diakonova *et al.*, 1987), in Turkmenia (Avdeev *et al.*, 1988) and many others. An example of how the thin sheet modelling and inversion work was presented in (Avdeev *et al.*, 1990a), where the main features of the MT field distribution at the South Turanian Plate and South Caspian Depression was explained (Figure 6). These features include the edge effect observed at the South Kara-Kum Platform for the telluric field orthogonal with respect to Kopet-Dagh mountains, significant depression of the electric field at the South Caspian Depression, magnetovariational anomaly beside Kopet-Dagh and so on. As a result, a crustal conductor was revealed under the Kopet-Dagh mountains, and the hypothesis on the possible existence of an astenospheric layer was proved.

Thin sheets can also be used to simulate electromagnetic fields induced in a model consisting of both surface and deep inhomogeneities. For example a preliminary model for the region of the EMSLAB experiment was presented in (Fainberg

Fig. 6. Comparison of experimental and theoretical curves at the South Turanian Plate and South Caspian Depression (Avdeev *et al.*, 1990a). (a) The South Slope of The Kara-Kum Platform, (b) Balhan and Western Kopetdagh zones, (c) Northern side of the South Caspian Depression, (d) South Caspian Depression, $\perp$ – transverse curves, $\|$ – longitudinal curves.

et al., 1988). The model consisted of two inhomogeneous layers embedded in the otherwise layered structure. The program used was based on the "Iterative Dissipative Method (IDM)" (Fainberg and Singer, 1980; Singer and Fainberg, 1985), and was able to carry out calculations on the mesh consisting of 10^4 nodes. At low frequencies simpler DC thin sheet programs can be useful to investigate the effects of local inhomogeneities (Hermance, 1982; Vanyan *et al.*, 1983; Barashkov A. S., 1988).

It should also be noted that problems similar to that of MT arise also in soundings with powerful controlled sources (Singer *et al.*, 1985; Kaikkonen *et al.*, 1987; Vanyan *et al.*, 1989a; Vanyan *et al.*, 1989b; Fainberg *et al.*, 1989). Topographic distortions have been modeled in (Dmitriev and Tavartkiladze, 1975; Tavartkiladze, 1975; Thayer, 1975; Jiracek and Holcombe, 1981; Holcombe, 1982; Mozley, 1982; Reddig and Jiracek, 1984; Reddig, 1984; Wannamaker *et al.*, 1986; Jiracek *et al.*, 1989).

3. The Validity Limits for Static Shift Correction Procedures and Spatial Filtering

This section is devoted to discussion of conditions which guarantee that the effect of surface inhomogeneities on electromagnetic fields reduces to static shift. Some analytical examples demonstrate the consequences which occur when the constraints are violated. The influence of spatial filtering on MT fields is also discussed.

3.1. The Adjustment Distance

The concept of adjustment distance is of great importance in any analysis of MT field distortions. It was shown in (Dmitriev, 1969; Ranganayaki and Madden, 1980) that B-polarized anomalous electric fields decay outside the surface anomaly in accordance with an exponential law, with the characteristic scale $\sqrt{ST}$. Here S is the surface layer conductance, and T is the transverse resistance of the intermediate high ohmic layer underlaid by a perfect conductor. The decay of the anomalous electric field was studied analytically by Dawson *et al.*, (1982) for a model consisting of two homogeneous half-sheets, overlaying the thin high ohmic layer underlaid by a uniform half space. It was shown in (Fainberg and Singer, 1987) that the toroidal part of the anomalous electric field decays outside the 3-D surface anomaly as $1/r^3$. The poloidal part decays as $K_1(r/\lambda_L)$, where K_1 is the McDonald's function and

$$\lambda_L = \sqrt{\frac{T}{S^{-1} + Z_0^-}}. \tag{5}$$

Here $Z_0^- = -\iota\omega\mu_0\lambda_0$ is the Tikhonov–Cagniard impedance of the laterally uniform medium underlying the surface layer. Equation (5) is valid for a layered underlying medium if $|\lambda_L| \gg |\lambda_0|$. The anomalous field amplitude depends on the

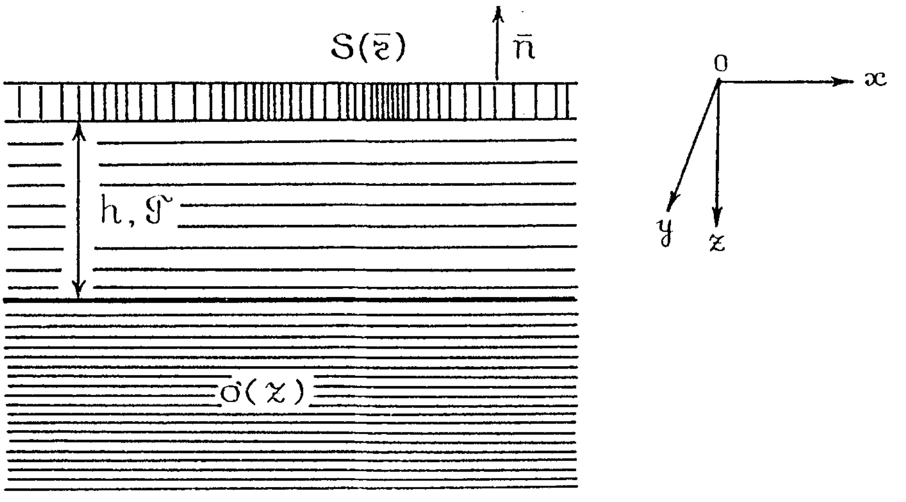

Fig. 7. Model with a non-uniform surface layer. $S(\mathbf{r})$ – surface conductance, h, T – thickness and transverse resistance of the intermediate layer, $\sigma(z)$ – the layered structure conductivity distribution.

conductivity distribution and the primary field polarization. Some examples are given below.

3.2. Static shift

We shall consider the model consisting of an inhomogeneous surface layer whose conductance is $S(x, y)$, and a laterally uniform underlying medium (Figure 7). The surface current distribution excited by an external field $\mathbf{j}^s$ satisfies the integral equation (Vasseur and Weidelt, 1977; Singer and Fainberg, 1985; Fainberg *et al.*, 1990a)

$$\mathbf{j}^s = \mathbf{j}_0^s - \hat{G}_0 * (S_0 R^* \mathbf{j}^s), \tag{6}$$

where "$*$" means the convolution operation,

$$R^* = 1/S - 1/S_0, \tag{7}$$

S_0 is some constant value and $\hat{G}_0$ is the tensor Green's function for a 1-D model consisting of the uniform surface layer with conductance S_0, and the same underlying structure as in the original model:

$$\hat{G}_0 = -(\mathbf{n} \times \nabla_\tau) \otimes (\mathbf{n} \times \nabla_\tau) Q_0^T - \nabla_\tau \otimes \nabla_\tau Q_0^P. \tag{8}$$

Here ∇_τ is the spatial differentiation operator with respect to lateral coordinates, $\mathbf{n}$ is the unit vector orthogonal to the earth's surface and directed outward and "$\otimes$" means the tensor product operation. Functions Q_0^T and Q_0^P are determined by expressions

$$\frac{\mathrm{d}}{\mathrm{d}r} Q_0^T = \int_0^\infty \frac{J_1(kr)}{1 - \iota\zeta_k} \frac{\mathrm{d}k}{4\pi}, \qquad \zeta_k = \frac{\omega\mu_0 S_0 \lambda_k}{1 + k\lambda_k}, \quad Z_k^T = -\iota\omega\mu_0\lambda_k, \tag{9}$$

$$\frac{\mathrm{d}}{\mathrm{d}r} Q_0^P = \int_0^\infty \frac{J_1(kr)}{1 - \iota S_0 Z_k^P} \frac{\mathrm{d}k}{4\pi},$$

where J_1 is a first order Bessel function, Z_k^T and Z_k^P are the spectral impedances of underlying structure for toroidal and poloidal modes.

It was shown by Singer and Fainberg (1985) that the Green's tensor possesses an important property. For an arbitrary vector $\mathbf{u} \in \mathbb{L}_2$ the norm

$$\|\hat{G}_0 * \mathbf{u}\| \leqslant \|\mathbf{u}\|. \tag{10}$$

This is valid for any value of S_0, but below the value

$$\frac{2}{S_0} = \frac{1}{S_{\min}} + \frac{1}{S_{\max}}.$$

is assumed. At low frequencies when

$$S_{\max} \cdot |Z_0^-| \ll 1, \tag{11}$$

the value $|\zeta_k| \leqslant S_0 \cdot |Z_0^-|$, and it can be shown that $S_0(Z_k^P - Z_0^-)$ is real and frequency independent. Hence the Green's function has a form

$$\hat{G}_0 = \hat{G}_0' + \hat{G}_0'',$$

where $\hat{G}_0'$ is real and frequency independent and $\|\hat{G}_0''\| \leqslant S_0 \cdot |Z_0^-|$. Designating $\hat{L}_0\mathbf{j}^s = \mathbf{j}^s + \hat{G}_0' *(S_0 R^* \mathbf{j}^s)$ one gets

$$\|\hat{L}_0\| \geqslant 1 - \frac{S_{\min}^{-1} - S_{\max}^{-1}}{S_{\min}^{-1} + S_{\max}^{-1}} = \frac{S_0}{S_{\max}}.$$

Hence Equation (6) reduces to

$$\mathbf{j}_s = \hat{L}_0^{-1}\mathbf{j}_0^s - \hat{\mathbf{L}}_0^{-1}\hat{G}_0'' * (S_0 R^* \mathbf{j}^s). \tag{12}$$

Taking into account that $\hat{L}_0$ does not depend on frequency and

$$\|\hat{L}_0^{-1} G_0'' *(S_0 R^* \mathbf{j}^s)\| \leqslant \frac{S_{\max}}{S_0} \cdot S_0 |Z_0^-| \cdot \|\mathbf{j}^s\| = S_{\max}\|Z_0^-\| \cdot \|\mathbf{j}^s\|,$$

one can easily see that the only frequency-dependent term in Equation (12) has a relative value smaller than $S_{\max}|Z_0^-|$, and therefore the frequency dependence of $\mathbf{j}^s$ is determined by $\mathbf{j}_0^s$, which in its turn is expressed via the normal field. Thus in the frequency band where $S_{\max}|Z_0^-| \ll 1$ the phase shift of the anomalous electric field with respect to the normal one is negligible. Further decrease in frequency does not affect the spatial distribution of the field. This means that the electric field measured at any point of the earth's surface differs from a normal one by a frequency independent factor. This corresponds to a vertical shift of apparent resistivity curves. The phase curves are unaffected.

The previous discussion shows that under certain conditions, the effect of local inhomogeneities as well as of geological noise can be suppressed by a plain vertical shift of the $\rho_a(T)$ curves on a logarithmic scale. The next question is how significantly can these conditions be softened. It is quite obvious that the 1-D character of the underlying structure as well as the restriction (11) on the frequency band are sufficient if they take place in a region exceeding the adjustment distance $|\lambda_L|$. The following examples show that violation of these conditions leads to the serious consequences.

3.2.1. *The Edge Effect*

Consider the case when the surface layer (Figure 7) consists of two uniform half planes, i.e.

$$S(x) = \begin{cases} S_0^l, & x < 0 \\ S_0^r, & x > 0 \end{cases}.$$

Then the apparent impedance of the B-polarized mode is distributed along the earth surface as

$$Z_a(x) = \begin{cases} Z_0^l \cdot \{1 + [\sqrt{(S_0^r Z_0^r)/(S_0^l Z_0^l)} - 1] \cdot \exp(+x/\lambda_L^l)\}, & x < 0 \\ Z_0^r \cdot \{1 + [\sqrt{(S_0^l Z_0^l)/(S_0^r Z_0^r)} - 1] \cdot \exp(-x/\lambda_L^r)\}, & x > 0 \end{cases},$$

where Z_0^l, Z_0^r are the left and right section impedances, λ_L^l, λ_L^r are the corresponding values of the "adjustment distance" (5). The apparent resistivity curves at different points of the profile are shown in Figure 8. It can be seen that the contact affects not only the vertical positions of the curves but also changes their form. The vertical shift is the only effect when condition (11) is satisfied for both conductive and resistive parts of the model. Thus Equation (11) should indeed be valid along the distance comparable with the "adjustment distance" to make sure that the $\rho_a(T)$ curve has undistorted form.

3.2.2. *The Deep S-effect*

The next point is now to show that the requirement of lateral uniformity for underlying structure is also necessary. If the underlying structure is laterally non-uniform, then the magnetic field which induces current in the surface layer has a frequency-dependent distribution. This can invalidate the static character of the surface effects in case of local inhomogeneities. The deep inhomogeneity can also cause nonstatic effects via galvanic interaction with the surface layer. A deep inhomogeneity can be the object of the survey, or it can also be an obstacle for the exploration of deeper layers. One can expect that the influence of small deep

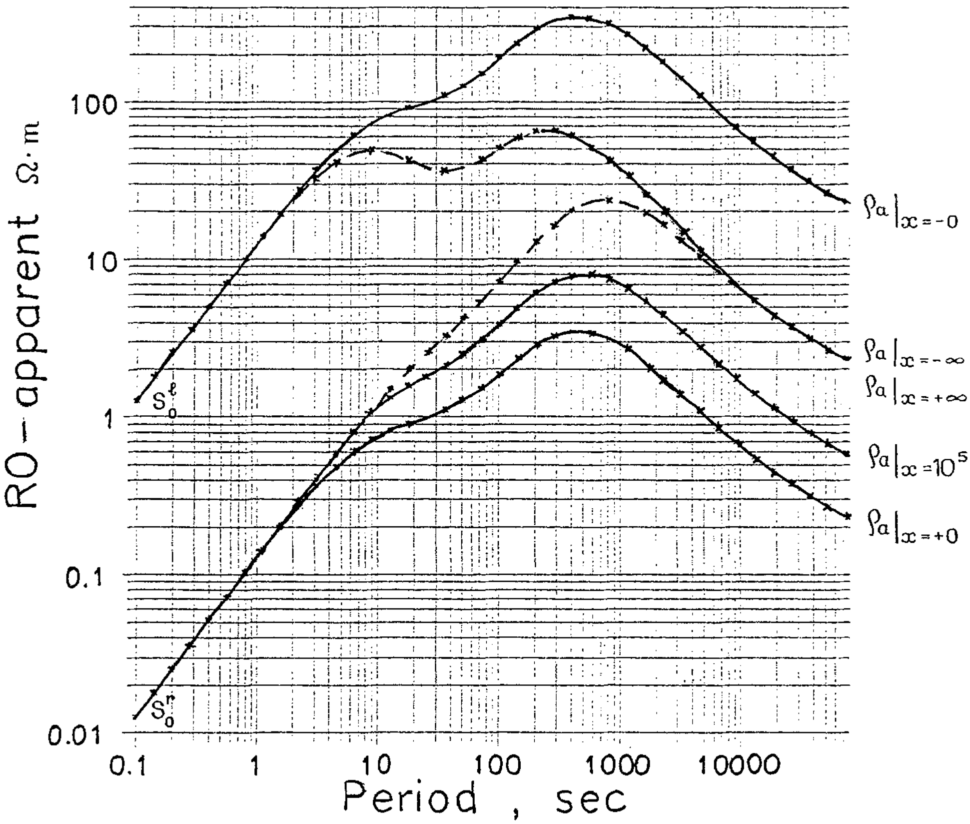

Fig. 8. The edge effect example. The model (Figure 7) parameters: $S_0(x) = \{100S, x < 0;\ 1000S, x > 0\}$, $\sigma(z) = \{10^{-4}\,\mathrm{S/m},\ 0 < z < h_1 = 10^4\,\mathrm{m};\ 10^{-1}\,\mathrm{S/m},\ 10^4\,\mathrm{m} < z < 1.5 \cdot 10^4\,\mathrm{m};\ 10^{-3}\,\mathrm{S/m},\ 1.5 \cdot 10^4\,\mathrm{m} < z < 7.5 \cdot 10^4\,\mathrm{m};\ 1\,\mathrm{S/m},\ 7.5 \cdot 10^4\,\mathrm{m} < z < \infty\}$. $\rho_a|_x$ – the apparent resistivity curve at point x.

inhomogeneities will not be noticeable at the earth's surface (Berdichevsky *et al.* 1982).

Against which parameter should the size of deep inhomogeneities be compared? The parameter should be bound with the distance along which "normalization" of the horizontal electric field (or decaying of vertical currents) takes place. From point of view it should be analogous to λ_L.

The model (Figure 9) we shall examine consists of two conductive thin sheets surrounding a resistive layer. The deep conductive layer is underlaid by another resistive layer and a laterally uniform conductive half space. If the surface conductive layer is uniform, i.e. $S_0(x)$ = Constant, and the deep layer has the conductance

$$S_1(x) = \begin{cases} S_1^i, & |x| < L \\ S_1^e, & |x| > L \end{cases},$$

and the condition

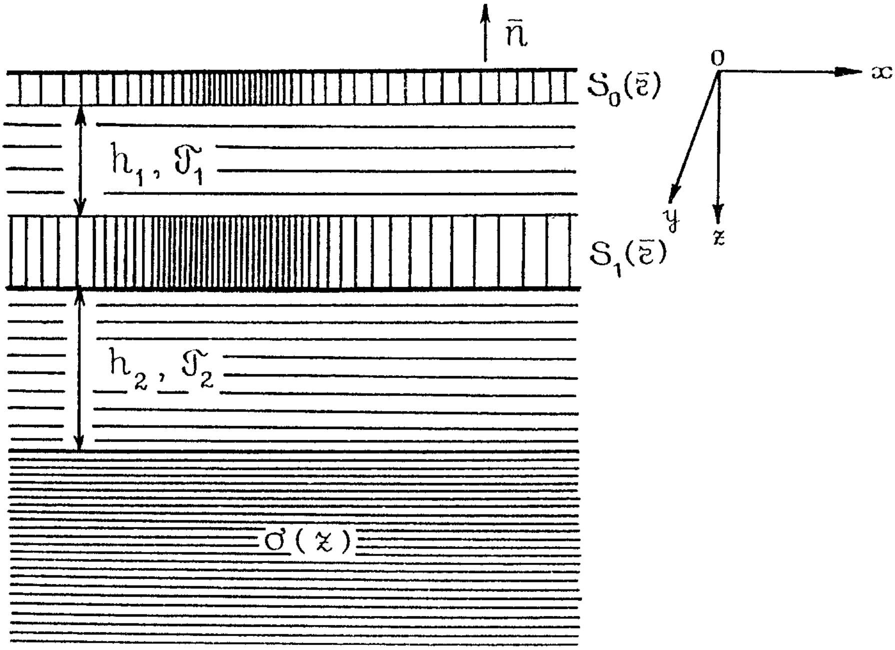

Fig. 9. The model with two conductive thin sheets.

$$2L \ll |\Lambda_L|, \qquad \Lambda_L = \sqrt{\frac{T_2}{S_1^{-1} + Z_1^-}},$$

(Z_1^- is the impedance of the medium underlying the deep conductive layer) is satisfied, then the apparent impedance of the B-polarized mode is

$$Z_a(x) = \begin{cases} \xi Z_0^i + \{Z_a(L) - \xi Z_0^i\} \cdot \dfrac{\cosh(x/\lambda_L^i)}{\cosh(L/\lambda_L^i)}, & |x| < L \\ Z_0^e + \{Z_0(L) - Z_0^e\} \cdot \exp(-|x| - L|/\lambda_L^e), & |x| > L \end{cases},$$

where Z_0^e is the impedance of the normal section and Z_0^i is the normal impedance of the section at point $x = 0$,

$$\lambda_L^i = \sqrt{\frac{T_1}{1/S_0 + 1/S_1^i - \iota\omega\mu_0 h_1}}, \qquad \lambda_L^e = \sqrt{\frac{T_1}{1/S_0 + 1/S_1^e - \iota\omega\mu_0 h_1}}, \tag{13}$$

$$Z_a(L) = \frac{Z_0^e/\lambda_L^e + Z_0^i/\lambda_L^i \cdot \tanh(L/\lambda_L^i)}{1/\lambda_L^e + 1/\lambda_L^i \cdot \tanh(L/\lambda_L^i)}, \tag{14}$$

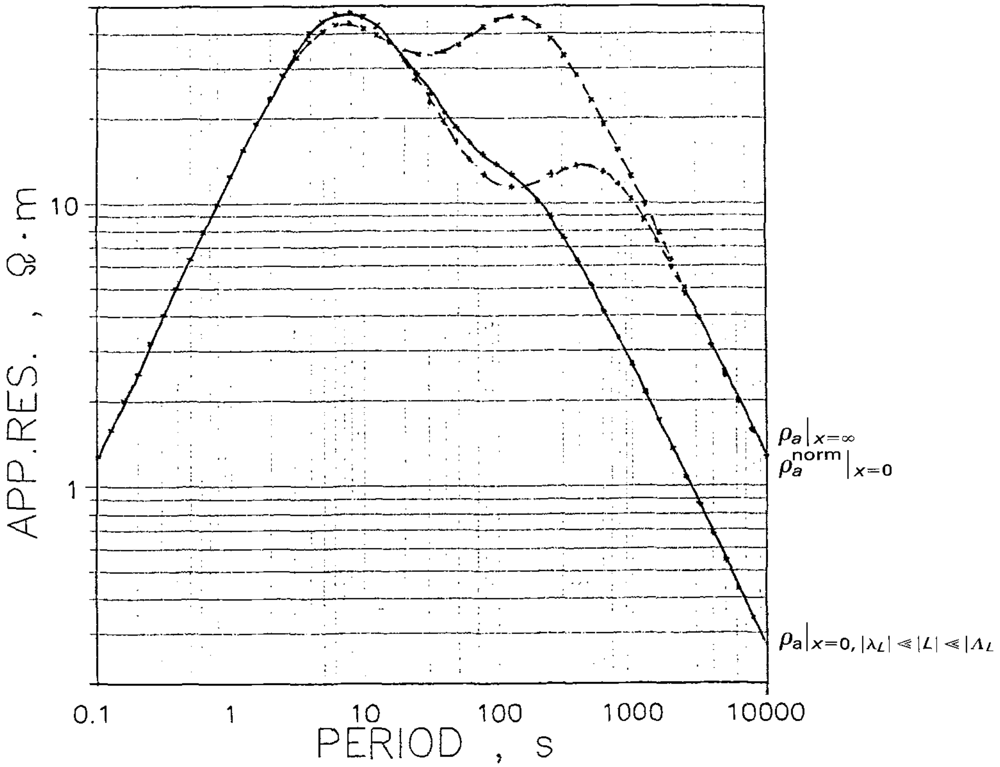

Fig. 10. The deep S-effect example. The earth model (Figure 9) parameters: $S_0 = 100$ S, $h_1 = 10^4$ m, $T_1 = 10^8\,\Omega \cdot \mathrm{m}^2$, $S_1^i = 2000$ S, $S_1^e = 500$ S, $L = 10^5$ m, $h_2 = 3 \cdot 10^4$ m, $T_2 = 3 \cdot 10^7\,\Omega \cdot \mathrm{m}^2$, $\sigma(z) = \infty$, $z > h_1 + h_2$. The apparent resistivity curves: $\rho_a|_{x=\infty}$ – the normal curve, $\rho_a^n|_{x=0}$ – the locally normal curve at point $x = 0$, $\rho_a|_{x=0, |\lambda_L| \ll L \ll |\Lambda_L|}$ – the curve at $x = 0$ in case of wide deep anomaly.

$$\xi = \frac{S_1^e Z_0^e (1/S_0 + 1/S_1^e - \iota\omega\mu_0 h_1) - \iota\omega\mu_0 h_1 (S_1^i - S_1^e)/S_0}{S_1^i Z_0^i (1/S_0 + 1/S_1^i - \iota\omega\mu_0 h_1)}, \tag{15}$$

and h_1 is the first resistive layer thickness. It should be noted that parameter ξ is equal to unity at frequencies higher than and including the second ascending branch.

It follows from Equation (14) that the effect of a small deep anomaly on the surface electric field is of order $L/|\lambda_L^i|$. From this point of view, deep geological noise does not exist. An example of the deep S-effect is shown in Figure 10. The shift of the second descending branch of the curve $\rho_a|_{x=0, L \gg |\lambda_L|}$ with respect to a normal curve is controlled by parameter ξ. As can be seen from Figure 10 the distortion of the apparent resistivity curve becomes static only when the low frequency band with respect to the deep inhomogeneity has been reached.

The previous examples make it possible to conclude that constraint (11) on the frequency band as well as the laterally uniform character of the underlying section should hold along a distance of the same order as the "adjustment distance". In this case the effect of local surface inhomogeneities on the telluric field reduces to the static one. It should be stressed here that this statement is valid for the local inhomogeneities. Analogous conditions for geological noise are much softer.

3.2.3. *2-D and 3-D Inhomogeneities*

In accordance with their definition, geological noise inhomogeneities are small in comparison with the effective penetration depth and with the "adjustment distance". Larger inhomogeneities were referred to as local and regional inhomogeneities. Field distributions along the earth's surface substantially differ for two and three dimensional inhomogeneities. Two following examples illustrate this circumstance.

In case of a 2-D model (Figure 7) with the surface layer conductance

$$S_0(x) = \begin{cases} S_0^i, & |x| < \alpha \\ S_0^e, & |x| > \alpha \end{cases}$$

the apparent impedance of the B-polarized mode is distributed along the surface in accordance with the law

$$Z_a(x) = \begin{cases} Z_0^i + \{Z_a(\alpha - 0) - Z_0^i\} \cdot \dfrac{\cosh(x/\lambda_L^i)}{\cosh(\alpha/\lambda_L^i)}, & |x| < \alpha \\ Z_0^e + \{Z_a(\alpha + 0) - Z_0^e\} \cdot \exp(-|\,|x|\text{-}\alpha\,|/\lambda_L^e), & |x| > \alpha \end{cases}, \tag{16}$$

where Z_0^e is the normal impedance, Z_0^i is the locally normal impedance for the area above the inhomogeneity, λ_L^i and λ_L^e are determined by Equation (5) after substitution of S_0 with S_0^i and S_0^e,

$$\frac{S_0^i}{S_0^e} \cdot Z_a(\alpha - 0) = Z_a(\alpha + 0) = Z_0^e \cdot \frac{1 + \lambda_L^i/\lambda_L^e \cdot \tanh(\alpha/\lambda_L^i)}{1 + \lambda_L^e/\lambda_L^i \cdot \tanh(\alpha/\lambda_L^i)}. \tag{17}$$

The following features of electric field distribution in the presence of 2-D surface inhomogeneities are displayed by these expressions.

1. The anomalous field amplitude over the inhomogeneity is determined by the ratio S_0^e/S_0^i. It can reach enormous values.

2. Apart from the inhomogeneity the anomalous field amplitude is dependent on the ratio α/λ_L^i in case of the conductive anomaly and on $\alpha \cdot \lambda_L^e/(\lambda_L^i)^2$ in case of the resistive one. The anomalous field decays in accordance with an exponential law with characteristic distance λ_L^e ($\alpha \ll |\lambda_L^i|$).

The picture is quite different in the case of an isometric surface inhomogeneity

$$S_0(r,\phi)=\begin{cases} S_0^i, & |r|<\alpha \\ S_0^e, & |r|>\alpha \end{cases}.$$

In the low frequency band the apparent impedance is

$$Z_a^{xy}(r,\phi)=Z_0^e\cdot\left\{1-\frac{\mathrm{d}f}{\mathrm{d}r}\cdot\cos^2\phi-\frac{f(r)}{r}\cdot\sin^2\phi\right\}, \tag{18}$$

$$Z_a^{yy}(r,\phi)=Z_0^e\cdot\left\{\frac{f(r)}{r}-\frac{\mathrm{d}f}{\mathrm{d}r}\right\}\cdot\sin\phi\cdot\cos\phi,$$

where

$$f(r)=\begin{cases} f_a I_1(r/\lambda_L^i)/I_1(\alpha/\lambda_L^i), & 0<r<\alpha \\ f_a K_1(r/\lambda_L^e)/K_1(\alpha/\lambda_L^e), & r>\alpha \end{cases}, \tag{19}$$

$$f_a=\{S_0^i-S_0^e\}\Bigg|\left\{\frac{S_0^i}{\lambda_L^i}\cdot\frac{I_1'(\alpha/\lambda_L^i)}{I_1(\alpha/\lambda_L^i)}-\frac{S_0^e}{\lambda_0^e}\cdot\frac{K_1'(\alpha/\lambda_L^e)}{K_1(a/\lambda_L^e)}\right\},$$

I_1 is the first order modified Bessel function. In case of a small inhomogeneity, whose size $a \ll \min\{|\lambda_L^i|, |\lambda_L^e|\}$ these expressions reduce to

$$f(r)=\begin{cases} f_a\cdot\dfrac{r}{\alpha}, & 0<r<\alpha \\ f_a\cdot\dfrac{\alpha}{r}, & r>\alpha \end{cases},\quad f_a=\alpha\cdot\frac{S_0^i-S_0^e}{S_0^i+S_0^e}.$$

Thus in case of a small surface inhomogeneity the anomalous electric field:

1. Is restricted for arbitrary values of S_0^i and S_0^e and
2. It decays outside the anomaly as $(\alpha/r)^2$.

This means that in order to find the electric field in the presence of small surface inhomogeneities one can restrict oneself to the problem of electromagnetic induction by a magnetic field specified by the undisturbed model (the model without the inhomogeneities mentioned above). Zero boundary condition for the anomalous field can be used at distances much greater than the anomaly size. This is valid in the frequency band where the anomaly does not affect the magnetic field, i.e. when the inductive effects originating from the excessive currents in the anomaly have terminated ($a\cdot\max\{\omega\mu_0 S, |\Lambda_0|\}\ll 1$). This is almost always valid for geological noise inhomogeneities in the MT frequency band. The static shift takes place independently of whether the undisturbed structure is one, two or three dimensional.

3.3. Spatal filtering

Due to surface inhomogeneities the electric field is nonuniform even when the primary field and an underlying medium are uniform. In such circumstances the spatial filtering method seems to be a natural remedy against distortions. How does the spatial filtering process affect MT data? This question is discussed below for the model shown in Figure 7.

The tangential components of the electric $\mathbf{E}_\tau$ and magnetic $\mathbf{H}_\tau^-$ fields at the surface of a laterally uniform medium (just under the surface layer) are related by the equation

$$\mathbf{n} \times \mathbf{H}_\tau^- = \hat{Y} * \mathbf{E}\boldsymbol{\tau} = \mathbf{E}_\tau / Z_0^- + \int_{\mathbb{R}^2} \hat{Y}(\mathbf{r} - \mathbf{r}')\{\mathbf{E}_\tau(\mathbf{r}) - \mathbf{E}_\tau(\mathbf{r}')\}\, \mathrm{d}s', \tag{20}$$

which can be deduced from a well known results of Dawson and Weaver (1979) and McKirdy *et al.* (1985). The admittance kernel $\hat{Y}$ was considered in (Avdeev *et al.*, 1989). It was shown that the toroidal part of the kernel decays exponentially with the characteristic distance determined by the effective penetration depth $|\lambda_0|$ ($Z_0^- = -\iota\omega\mu_0\lambda_0$ is the Tikhonov–Cagniard impedance of the underlying section). The poloidal part also decays exponentially but along the distance $|\sqrt{T/Z_0^-}|$, where T is the transverse resistance of the section.

If the electromagnetic field changes significantly only along distances greater than the adjustment distance, the second term in Equation (20) can be omitted, and Equation (20) reduces to the Leontovich's expression. If the field changes are more rapid, then high spatial harmonics can be suppressed using the spatial filtering process, so that the filtered field would satisfy the equation

$$\mathbf{n} \times \langle \mathbf{H}_\tau^- \rangle_\mathbf{r} = \langle \mathbf{E}_\tau \rangle_\mathbf{r} / Z_0^- . \tag{21}$$

Taking into account that the tangential magnetic fields at the earth's surface and just under the surface layer satisfy the equation

$$\mathbf{n} \times (\mathbf{H}_\tau - \mathbf{H}_\tau^-) = S \cdot \mathbf{E}_\tau,$$

one can easily find the expression for the filtered field

$$\mathbf{n} \times \langle \mathbf{H}_\tau \rangle_\mathbf{r} = \langle \mathbf{E}_\tau \rangle_\mathbf{r} \cdot \langle 1/Z_0 \rangle_\mathbf{r} + \mathbf{Q}(\mathbf{r}). \tag{22}$$

Here the averaged admittance and the bias are defined as

$$\langle 1/Z_0 \rangle_\mathbf{r} = 1/Z_0^- + \langle S \rangle_\mathbf{r}, \tag{23}$$

$$\mathbf{Q}(\mathbf{r}) = \langle S \cdot \mathbf{E}_\tau \rangle_\mathbf{r} - \langle S \rangle_\mathbf{r} \cdot \langle \mathbf{E}_\tau \rangle_\mathbf{r}. \tag{24}$$

Thus the bias is determined by the correlation between $S(\mathbf{r})$ and $\mathbf{E}_\tau(\mathbf{r})$, and can be evaluated using experimental data. If the bias is small in comparison with $\langle \mathbf{E}_\tau \rangle_\mathbf{r} \langle 1/Z_0 \rangle_\mathbf{r}$ then Equation (22) reduces to the Leontovich's expression. It follows

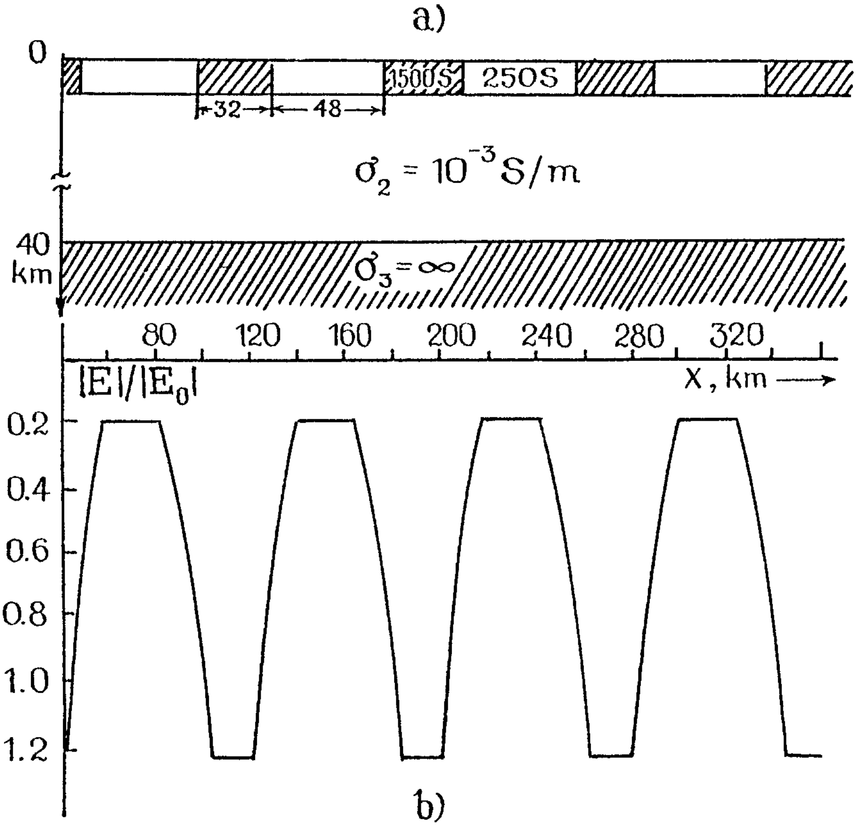

Fig. 11. Example of local distortions of MT field. (a) The model geometry, (b) Distribution of the B-polarized electric field, T = 1000 s.

from Equation (24) that **Q** is restricted by the relative deposit of surface currents into the magnetic field. Hence the bias should disappear in the low frequency branch of the MT band.

The 2-D model displayed in Figure 11a includes a surface layer consisting of stripes with width 48 and 32 km and conductances 250 and 1500 S. The resistive layer has thickness 40 km and specific conductivity 10^{-3} S/m, the deeper half space is occupied by a perfect conductor. The B-polarized electric field distribution shown in Figure 11b displays the "classical" S-effect. The apparent resistivity curve calculated using the averaged field is shown in Figure 12 (Avdeev *et al.*, 1990b) together with the curve corresponding to the averaged value $\langle S \rangle = 750$ S. The descending branches of both curves coincide. The most significant discrepancy takes place at the ascending branch and near the maximum of the normal curve. In the example both curves are conformal but this is not a general rule.

The bias depends on the definition of the averaged impedance. It was proposed in (Dmitriev and Berdichevsky, 1988) to assume

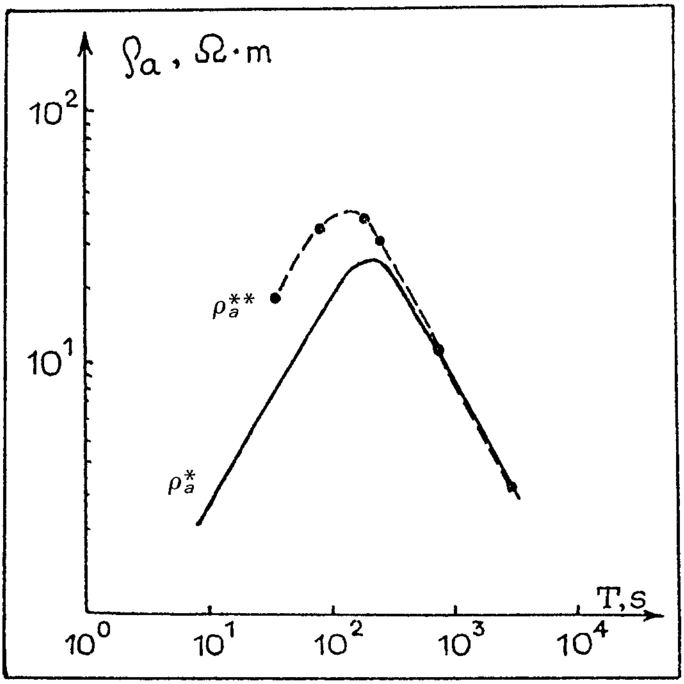

Fig. 12. The result of spatial filtering for a model in Figure 11. ρ_a^* – the normal curve corresponding to $\langle S \rangle = 750$ S, ρ_a^{**} – the curve calculated using the averaged field.

$$1/\langle Z_0 \rangle_{\mathbf{r}} = 1/Z_0^- + \langle 1/S \rangle_{\mathbf{r}}. \tag{25}$$

In this case the bias is equal to

$$\mathbf{Q}(\mathbf{r}) = \langle S \cdot \mathbf{E}_\tau \rangle_{\mathbf{r}} - \langle 1/S \rangle_{\mathbf{r}}^{-1} \cdot \langle \mathbf{E}_\tau \rangle_{\mathbf{r}}. \tag{26}$$

This value can be neglected if the surface current is constant along the area covered by the filter. This takes place when such effects as current channeling, flowing around as well as leakage of currents can be omitted. As to geological noise, any bias originating from filtering is usually negligible as the MT frequency band belongs to the low frequency band with respect to the geological noise inhomogeneities.

4. Conclusion

Before terminating the review, it seems reasonable to clarify what one has in mind when speaking about distortions.

4.1. Geological noise

First of all we had in mind the effects due to small uncontrollable surface inhomogeneities, which were referred to as geological noise. Therefore the electromagnetic fields which would be observed in the absence of geological noise were considered as undistorted fields. Commonly speaking these fields are three dimensional, and they display information on deep and large scale (local and regional) surface inhomogeneities.

Nowadays the problem of geological noise looks even more significant than ever before. There exist now tools for data acquisition and processing which guarantee several percent accuracy in data. At the same time the data are often contaminated by the noise on several hundred or even thousand percents. Due to the ill posed character of the inverse problem, results of interpretation can appear much more contaminated or even erroneous. Fortunately the static effects are the main effects originating from the geological noise.

The static shift correction procedure based on auxiliary TEM soundings seems to be very promising, as it should not be too expensive. It can be used for correction of apparent resistivity curves as well as in distortion tensor tecniques. The most consistent approach should employ the field affected by large scale inhomogeneities (local and regional) as the undistorted fields.

Another approach based on the random nature of geological noise is spatial filtering of the electric field. The areal modification of EMAP would indeed be able to suppress the geological noise effects (Jiracek, 1990; Andrieux, pers. comm., 1990), but it is important to preserve such extremely important features of the EMAP approach as antialising. One of the important results of the approach is designing acquisition equipment which promises to bring synchronous areal measurements into reality. The importance of this point can not be overestimated. Even if the data acquisition, processing and distortion correction were carried out with no errors, it would not mean that the resultant data are sufficient for interpretation of 3-D electromagnetic fields. On the other hand, if synchronous measurements are available, the magnetic field measurements will often provide the same information free of geological noise effects. Even such parameters as the transverse resistance can be inferred from magnetic observations (Fainberg *et al.*, 1990b).

In 2-D situations contaminated by geological noise inhomogeneities the decomposition approach of Groom and Bailey (1989), combined with static corrections of the mean impedances, also looks very attractive.

It should be noted that the most attractive feature of magnetotellurics is a chance to make inferences from single point observations. The method of spatial derivatives (Berdichevsky *et al.*, 1969; Kuckes, 1973; Fainberg and Berdichevsky, 1977) has the same feature. The apparent impedance determined by the method is much less affected by surface inhomogeneities than the MT impedance and may provide correct results even when significant galvanic distortions exist (Fainberg and Singer, 1987). Therefore designing of experimental equipment for measurements of the magnetic field derivatives would have rich future.

4.2. Local inhomogeneities

The term "distortions" has quite another meaning for local inhomogeneities. In this case distortion means deflection of the curve from the locally normal curve. The problem to restore the locally normal curve from the distorted one is strictly speaking insoluble. It can be solved approximately and use only for rough preliminary interpretation. As it was shown in Section 3.2, local distortions reduce to static shift only when rather hard conditions are satisfied in the vicinity of the observation point. The size of this vicinity is controlled by the effective penetration depth in case of E-polarized field and by the "adjustment distance" in case of the B-polarized or 3-D field. The period should correspond to the low frequency band and the underlying medium should be one dimensional in this vicinity.

In other words the methods used as remedies against geological noise have only limited application against local inhomogeneities. Results of their application are of limited accuracy. The only tool is modelling. Although an enormous amount of information is necessary to carry out the modelling, this corresponds to physical essence of the phenomenon and can not be bypassed on the final stage of interpretation at least. Concerning local distortions the synchronous measurements could also provide the information necessary for more sophisticated methods of interpretation (Berdichevsky and Zhdanov, 1984; Avdeev *et al.*, 1986).

Acknowledgements

The author is grateful to all colleagues who responded to his call for references and papers. My greatest gratitude is addressed to E. Fainberg whose influence on my scientific position was always very significant. I deeply appreciate the remarks and recommendations of A. Jones, A. Schultz, P. Andrieux and two referees who helped me to improve the paper.

References

Andrieux, P. and Wightman, W. E.: 1984, 'The So-called Static Correction in Magnetotelluric Measurements', *54th Ann. Internat. Mtg., Soc. Explor. Geophys.*, Expanded Abstracts, pp. 43–44.

Avagimov, A. A., Ashirov, T., Berdichevsky, M. N., Dubrovsky, V. G., Dubrovskaia, E. V., Iliamanov, K., Lagutinskaia, L. P., Nepesov, K., Smirnov, Ia. B., Sopiev, V. A., Tavnelova, O. M., and Fainberg, E. B.: 1981, 'Geoelectrical and Thermal Model of Deep Structure of South of Turanian Plate (in Russian)', *Izv. Akad. Nauk SSSR Fiz. Zemli* **7**, 15–28.

Avdeev, D. B., Singer, B. Sh., and Fainberg, E. B.: 1986, 'The Inverse Problem of Geoelectrics for Thin Sheet Models (in Russian)', in *Fundamental Problems of Marine Electromagnetic Explorations*, Moscow, IZMIRAN, p. 24–47.

Avdeev, D. B., Fainberg, E. B., Singer, B. Sh., Avagimov, A. A., and Dubrovsky, V. G.: 1988, 'The Thin Sheet Interpretation of the Deep Electromagnetic Sounding in Turkmenia', *9th Workshop on EM induction in the Earth and Moon*, Abstracts, 2.5.

Avdeev, D. B., Fainberg, E. B., and Singer, B. Sh.: 1989, 'On Applicability of the Tikhonov-

Cagniard's Magnetotelluric Model for Sounding of a Non-uniform Medium', *Phys. Earth Planet. Inter.* **53**, 343–349.

Avdeev, D. B., Dubrovsky, V. G., Fainberg, E. B., Pankratov, O. V., and Singer, B. Sh.: 1990a, 'Deep Electromagnetic Investigations at the South of Turanian Plate', *10th Workshop on EM Induction in the Earth*, 5.9.

Avdeev, D. B., Godneva, G. S., Singer, B. Sh., and Fainberg, E. B.: 1990b, 'The Spatial Filtering of Local Distortions of Magnetotelluric Field', *Izv. Akad. Nauk SSSR Fiz. Zemli* **10**, 3–11.

Barashkov, A. S.: 1988, 'Low-Frequency Asymptotic for a Solution of the Three-Dimensional MTS Problem (in Russian)', *Izv. Akad. Nauk SSSR Fiz. Zemli* **2**, 90–100.

Bahr, K.: 1985, 'Magnetotellurische Messung des Elektrischen Widerstandes der Erdkruste und des Oberen Mantels in Gebieten mit Lokalen und Regionalen Leitfahigkeitsanomalien', Ph.D. Thesis, Univ. of Gottingen.

Berdichevsky, M. N., Vanyan, L. L., and Fainberg, E. B.: 1969, 'Magnetovariational Sounding Based on the Spatial Derivatives of Field (in Russian)', *Geomagnetizm i Aeronomia* **1**, 369–371.

Berdichevsky, M. N. and Nechaeva, G. P.: 1975, 'Reduction of Local Distortions in Magnetotelluric Soundings (in Russian)', *Prikladnaya Geofizika* **79**, 87–96.

Berdichevsky, M. N. and Dmitriev, V. I.: 1976a, 'Distortion of Magnetic and Electric Fields by Near-Surface Lateral Inhomogeneities', *Acta Geod., Geophys. Montanist. Acad. Sci. Hung.* **11**, 447–483.

Berdichevsky, M. N. and Dmitriev, V. I.: 1976b, 'Basic Principles of Interpretation of Magnetotelluric Sounding Curves', in *Geoelectric and Geothermal Studies, KAPG Geophysical Monograph.*, Akademiai Kiado, Budapest, pp. 165–221.

Berdichevsky, M. N., Vanyan, L. L., Kuznetsov, V. A., Levadny, V. T., Mandelbaum, M. M., Nechaeva, G. P., Okulessky, B. A., Shylovsky, P. P., and Shpak, I. P.: 1980, 'Geoelectrical Model of the Baikal Region', *Phys. Earth Planet. Inter.* **22**, 1–11.

Berdichevsky, M. N., Dmitriev, V. I., Barashkov, I. S., Mershikova, N. A., and Kobzova, V. M.: 1982, 'On Magnetotelluric Sounding of Conductive Zones in the Crust and Upper Mantle (in Russian)', *Izv. Akad. Nauk SSSR Fiz. Zemli* **7**, 55–68.

Berdichevsky, M. N., Dmitriev, V. I., Barashkov, I. S., and Lebedeva, N. A.: 1984, 'Magnetotelluric Sounding of Crust Conductive Zones (in Russian)', *Izv. Akad. Nauk SSSR Fiz. Zemli* **9**, 50–56.

Berdichevsky, M. N. and Zhdanov, M. S.: 1984, *Advanced Theory of Deep Geomagnetic Sounding*, Elsevier Sci. Pub., Amsterdam, 408 pp.

Berdichevsky, M. N., Dmitriev, V. I., Feldman, I. S., Berezina, N. I., Demidov, A. I., and Yakovlev, S. P.: 1988, 'Interpetetation of Deep MT-soundings in Tungus Sineclise (in Russian)', *Izv. Akad. Nauk SSSR Fiz. Zemli* **7**, 73–79.

Berdichevsky, M. N., Vanyan, L. L., and Dmitriev, V. I.: 1989, 'Methods Used in USSR to Reduce Near-Surface Inhomogeneity Effects on Deep Magnetotelluric Sounding', *Phys. Earth Planet. Inter.* **53**, 194–206.

Bostick, F. X.: 1977, 'A Simple Almost Exact Method of MT Analysis', *Workshop on Electrical Methods in Geothermal Exploration*, Univ. of Utah Res. Inst., U.S. Geol. Surv. Contract 14-08-0001-g-359, pp. 174–183.

Bostick, F. X.: 1984, 'Electromagnetic Array Profiling Survey Method', US Patent 4.591,791, dated May 27th 1986, filed July 31, 1986.

Bostick, F. X.: 1986, 'Electromagnetic Array Profiling (EMAP)', *56th Ann. Internat. Mtg., Soc. Explor. Geophys.*, Expanded Abstracts, pp. 60–61.

Chouteau, M. and Bouchard, K.: 1988, 'Two-Dimensional Terrain Corrections in Magnetotelluric Survey', *Geophysics* **6**, 854–862.

Dawson, T. W. and Weaver, J. T.: 1979, 'Three-Dimensional Electromagnetic Induction in a Non-uniform Thin Sheet at the Surface of Uniformly Conducting Earth', *Geophys. J. R. Astr. Soc.* **59**, 445–462.

Dawson, T. W., Weaver, J. T., and Raval, U.: 1982, 'B-Polarization Induction in Two Generalized Thin Sheets at the Surface of a Conducting Half-Space', *Geophys. J. R. Astr. Soc.* **69**, 209–234.

Diakonova, A. G., Godneva, G. S., and Fainberg, E. B.: 1987, 'On the Electrical Conductivity of the Upper Mantle of the Ural Region (in Russian)', in *Solution of the Direct and Inverse Problems of Geoelectrics*, Moscow, IZMIRAN, pp. 108–123.

Dmitriev, V. I.: 1969, 'Electromagnetic Fields in Inhomogeneous Media (in Russian)', *Trudy VC MGU*, Moscow, MGU, 131 pp.

Dmitriev, V. I. and Tavartkiladze, Sh. A.: 1975, 'Investigation of the Earth Surface Uplift Effect on the Deep Magnetotelluric Sounding (in Russian)', in *Electromagnetic Sounding of the Earth and Moon*, Moscow, MGU, pp. 36–48.

Dmitriev, V. I. and Berdichevsky, M. N.: 1988, 'The Statistical Model of the S-Effect', *9th Workshop on EM induction in the Earth and Moon*, Abstracts, 1.13.

Dosso, H. W., Nienaber, W., and Chen, J.: 1989, 'Laboratory Electromagnetic Modelling of the Subducting Juan de Fuca Plate', *Phys. Earth Planet. Inter.* **53**, 221–227.

Druskin, V. L. and Knizhnerman, L. A.: 1988, 'Spectral Finite-Difference Method for Numerical Solution of Three-Dimensional Nonstationary Problems in Electrical Prospecting (in Russian)', *Izv. Akad. Nauk SSSR Fiz. Zemli* **8**, 63–74.

Fainberg, E. B. and Berdcichevsky, M. N.: 1977, 'Deep Magnetovariation Profiling with the Method of Derivatives', *Acta Geodaet., Geophys. Montanist. Acad. Sci. Hung.* **12**(1–3), 377–391.

Fainberg, E. G. and Singer, B. Sh.: 1980, 'Electromagnetic Induction in a Non-uniform Spherical Model of the Earth', *Ann. Geophys.* **36**, 127–134.

Fainberg, E. B.: 1983a, 'Global and Regional Magnetovariational Sounding of the Earth (in Russian)', Dr.Sc. Thesis, Moscow, IZMIRAN.

Fainberg, E. B.: 1983b, 'Global Deep Sounding (in Russian)', in *Mathematical Modelling of Electromagnetic Fields*, Moscow, IZMIRAN, pp. 79–121.

Fainberg, E. B. and Singer, B. Sh.: 1987, 'The Influence of Surface Inhomogeneities on Deep Electromagnetic Soundings of the Earth', *Geophys. J. R. Astr. Soc.* **90**, 61–73.

Fainberg, E. B., Godneva, G. S., Pankratov, O. V., Singer, B. Sh., and EMSLAB Group: 1988, 'Thin-Sheet Modelling of Electromagnetic Fields in EMSLAB Experiment', *9th Workshop on EM Induction in the Earth and Moon*, Abstracts, 10.12.

Fainberg, E. B., Singer, B. Sh., and Godneva, G. S.: 1989, 'Thin Sheet Modelling of the Alternating Electromagnetic Field (in Russian)', in *Geoelectrical Investigations with a Powerful Current Source on the Baltic Shield*, Moscow, Nauka, pp. 141–149.

Fainberg, E. B., Kuvshinov, A. V., and Singer, B. Sh.: 1990a, 'Electromagnetic Induction in a Spherical Earth with Non-uniform Oceans and Continents in Electric Contact with the Underlying Medium – I. Theory, Method and Example', *Geophys. J. Int.* **102**, 273–282.

Fainberg, E. B., Kuvshinov, A. V., and Singer, B. Sh.: 1990b, 'Electromagnetic Induction in a Spherical Earth with Non-uniform Oceans and Continents in Electric Contact wiht the Underlying Medium – II. Bimodal Global Geomagnetic Sounding of the Lithosphere', *Geophys. J. Int.* **102**, 283–286.

Groom, R. W. and Bailey, R. C.: 1989, 'Decomposition of Magnetotelluric Impedance Tensors in the Presence of Local Three-Dimensional Galvalic Distortion', *J. Geophys. Res.* **94**, 1913–1925.

Hempfling, R.: 1977, 'Beobachtung und Auswertung Tagesperiodischer Variationen des Erdelektrischen Feldes in der Umgebung von Gottingen', Ph.D. Thesis, Univ. of Gottingen.

Hermance, J. F.: 1982, 'The Asymptotic Response of Three-Dimensional Basin Offsets to Magnetotelluric Fields at Long Periods: The Effects of Current Channeling', *Geophysics* **47**, 1562–1573.

Holcombe, H. T.: 1982, 'Terrain Effects in Resistivity and MT Surveys', Ph.D. Thesis, Univ. of New Mexico.

Hohmann, G. W.: 1975, 'Three-Dimensional Induced Polarization and Electromagnetic Modelling', *Geophysics* **40**, 309–324.

Hvozdara, M.: 1981, 'EM Induction of a Three-Dimensional Inhomogeneity in the Two-Layered Earth. Parts 1', *Studia Geoph. et Geod.* **25**, 167–180.

Jiracek, G. R. and Holcombe, H. T.: 1981, 'Evaluation of Topographic Effects in Magnetotelluric Using a Modified Rayleigh Technique', *51st. Ann. Internat. Mtg., Soc. Explor. Geophys.*

Jiracek, G. R., Reddig, R. P., and Kojima, R. K.: 1989, 'Application of the Rayleigh – FFT Technique to the Magnetotelluric Modelling and Correction', *Phys. Earth Planet. Inter.* **53**, 365–375.

Jiracek, G. R.: 1990, 'Near-Surface and Topographic Distortion in Electromagnetic Induction', *Surveys in Geophysics* **11**, 163–203.

Jones, A. G.: 1983, 'The Problem of Current Channeling: a Critical Review', *Geophys. Surv.* **6**, 79–122.

Jones, A. G.: 1988, 'Static Shift of Magnetotelluric Data and Its Removal in a Sedimenary Basin Environment', *Geophysics* **53**, 967–978.

Jones, A. G., Boerner, D. E., and Kurtz, R. D.: 1989, 'EMAP Data Processing in the Warenumber Domain', Contributed paper at 1989 SEG Mtg.

Junge, A.: 1986, 'Zur Messung und Deutung der Halbmondentagigen Variation des Erdelectrischen Feldes in Nord- und WestDeutschland', Ph.D. Thesis, Univ. of Gottingen.

Junge, A.: 1988, 'The Telluric Field in Northern Germany Induced by Tidal Motion in the North Sea', *Geoph. J.* **95**, 523–533.

Kaikkonen, P., Vanyan, L. L., Demidova, T. A., Yegorov, I. V., and Palshin, N. A.: 1987, 'Numerical Modelling of Deep Dipole-Dipole MHD Sounding', *Phys. Earth Planet. Inter.* **50**, 226–229.

Kaufmann, A. A.: 1988, 'Reduction at the Geological Noise in Magnetotelluric Soundings', *Geoexploration* **25**, 145–161.

Kuckes, A. B.: 1973, 'Relation Between Electrical Conductivity of a Mantle and Fluctuating Magnetic Fields', *Geophys. J. Roy. Astr. Soc.* **32**, 119–131.

Larsen, J. C.: 1977, 'Removal of Local Surface Conductivity Effects from Low Frequency Mantle Response Curves', *Acta Geod., Geophys. Montanist. Acad. Sci. Hung.* **12**, 183–186.

Menvielle, M.: 1988, 'Effects of Crustal Conductivity Heterogeneities on the Electromagnetic Field', *Surveys in Geophysics* **9**, 319–348.

McKirdy, D. McA., Weaver, J. T., and Dawson, T. W.: 1985, 'Induction in a Thin Sheet of Variable Conductance at the Surface of a Stratified Earth – II. Three-Dimensional Theory', *Geophys. J. R. Astr. Soc.* **80**, 177–194.

Moroz, I. P., Kobzeva, V. M., and Timoshin, B. V.: *Modelling of Electrodynamic Processes in Non-uniform Conductive Media* (in Russian), Kiev, Nauk. Dumka, 88 pp.

Mozley, E. C.: 1982, 'An Investigation of the Conductivity Distribution in the Vicinity of a Cascade Volcano', Ph.D. Thesis, Univ. of California, Berkeley.

Newman, G. A.: 1989, 'Deep Transient Electromagnetic Sounding with a Grounded Source over Near-Surface Conductors', *Geophys. J. Int.* **98**, 587–601.

Park, S. K.: 1985, 'Distortion of Magnetotelluric Sounding Curves by Three-Dimensional Structures', *Geophysics* **50**, 785–797.

Pellerin, L. and Hohmann, G. W.: 1990, 'Transient Electromagnetic Inversion: a Remedy for Magnetotelluric Static Shifts', *Geophysics* **55**, 1242–1250.

Poll, H. E., Weaver, J. T., and Jones, A. G.: 1989, 'Calculation of Voltages for Magnetotelluric Modelling of a Region with Near-Surface Inhomogeneities', *Phys. Earth Planet. Inter.* **53**, 287–297.

Raiche, A. P.: 1974, 'An Integral Equation Approach to 3-D Modelling', *Geoph. J. R. Astr. Soc.* **55**, 507–511.

Ranganayaki, R. P. and Madden, T. R.: 1980, 'Generalized Thin Sheet Analysis in Magnetotellurics: an Extension of Price's Analysis', *Geophys. J. R. Astr. Soc.* **60**, 445–457.

Reddig, R. P.: 1984, 'Application of the Rayleigh – FFT Technique to Topographic Corrections in MT', M.S. Thesis, San. Diego State Univ.

Reddig, R. P. and Jiracek, G. R.: 1984, 'Topographic Modelling and Correction in Magnetotellurics', *54th Ann. Internat. Mtg., Soc. Explor. Geophys.*, Expanded Abstracts, pp. 44–47.

Robertson, R. C.: 1988, 'The Electromagnetic Response of a Heterogenous Layer Modeled by Two Thin Sheets in a Uniformly Conducting Half-Space', *IEEE Trans. Geosci. Rem. Sensing* GE**26**, 2–10.

Rokityansky, I. I.: 1982, 'Geoelectric Investigation of the Earth's Crust and Mantle', Springer-Verlag, Berlin, 381 pp.

Schmucker, U.: 1970, 'Anomalies of Geomagnetic Variations in the Southern United States', Scripps Institution of Oceanography Bull. **13**, Univ. of California Press, 165p.

Shoemaker, C. L., Shoham, Y., and Hockey, R. L.: 1986, 'Interpretation of Natural Source Electromagnetic Array Data', *56th Ann. Internat. Mtg., Soc. Explor. Geophys.*, Expanded Abstracts, pp. 63–65.

Singer, B. Sh., Dubrovsky, V. G., Fainberg, E. B., Berdychevsky, M. N., and Iliamanov, K.: 1984, 'Quasi-Tree-Dimensional Modelling of Magnetotelluric Fields on the South of Turanian Plate and in the South-Caspian Depression (in Russian)', *Izv. Akad. Nauk SSSR Fiz. Zemli*, **1**, 69–81.

Singer, B. Sh. and Fainberg, E. B.: 1985, *Electromagnetic Induction in Non-uniform Thin Sheets* (in Russian), Moscow, IZMIRAN, 234 pp.

Singer, B. Sh., Fainberg, E. B., and Vasilieva, T. A.: 1985, 'Modelling of MHD-Field on the Kola Peninsula (in Russian)', in *Electromagnetic Sounding of the Earth*, Moscow, IZMIRAN, pp. 78–87.

Sternberg, B. K., Buller, P. L., Kasabeth, J. L., and Mehreteat, E.: 1982, 'Electrical Methods for Hydrocarbon Exploration: II, Magnetotelluric (MT) Methods: Proc. Southern Methodist Univ. Simpos., III, Unconventional Methods in Exploration for Petroleum and Natural Gas, SMU Press, 1984, pp. 202–230.

Sternberg, B. K., Washburne, J. C., and Pellerin, L.: 1988, 'Correction for the Static Shift in Magnetotellurics Using Transient Electromagnetic Sounding', *Geophysics* **53**, 1459–1468.

Tavartkiladze, Sh. A.: 1975, 'Investigation of the Earth Surface Depression Effect on the Deep Magnetotelluric Sounding (in Russian)', in *Electromagnetic Sounding of the Earth and Moon*, Moscow, MSU, pp. 49–61.

Thayer, R. E.: 1975, 'Topographic Distortion at Telluric Currents: A Simple Calculation', *Geophysics* **40**, 91–95.

Ting, S. C. and Hohmann, G. M.: 1981, 'Integral Equation Modelling of Three-Dimensional Magnetotelluric Response', *Geophysics* **46**, 182–197.

Torres-Verdin, C.: 1985, 'Implication of the Born Approximation for MT Problem in Three-Dimensional Environments', M.S. Thesis, Univ. of Texas.

Vanyan, L. L., Berdichevsky, M. N., Fainberg, E. B., and Fiskina, M. V.: 1977, 'The Study of the Asthenosphere of the East-European Platform by Electromagnetic Sounding', *Phys. Earth Planet. Inter.* **14**, 1–2.

Vanyan, L. L., Berdichevsky, M. N., Vasin, N. K., Okulessky, B. A., and Shilovsky, P. P.: 1980, 'On Normal Geoelectrical Cross-Section (in Russian)', *Izv. Akad. Nauk SSSR Fiz. Zemli* **2**, 73–76.

Vanyan, L. L., Dubrovsky, V. G., Yegorov, I. V., and Konnov, Yu. K.: 1983, 'Structure of the Low-Frequency Telluric Field in the South Caspian Megadepression in Accordance with Numerical Modelling (in Rusian)', *Izv. Akad. Nauk SSSR Fiz. Zemli* **7**, 98–101.

Vanyan, L. L., Debabov, A. S., and Yudin, M. N.: 1984, *Interpretation of Magnetotelluric Sounding of Inhomogeneous Media* (in Russian), Moscow, Nedra, 194 pp.

Vanyan, L. L., Demidova, T. A., Palshin, N. A., Zhamaletdinov, A. A., Kuksa, Yu. I., Kaikkonen, P., and Korja, T.: 1989a, 'Interpretation of Deep DC Soundings in the Baltic Shield', *Phys. Earth Planet. Inter.* **54**, 149–155.

Vanyan, L. L., Demidova, T. A., Yegorov, I. V., and Palshin, N. A.: 1989b, 'Thin Sheet Modelling of the DC Electric Field (in Russian)', in *Geoelectrical Investigation with a Powerful Current Source on the Baltic Shield*, Moscow, Nauka, pp. 133–141.

Vasseur, G. and Weidelt, P.: 1977, 'Bimodal Electromagnetic Induction in Non-uniform Thin Sheets with Application to the Northern Pyrenean Anomaly', *Geophys. J. R. Astr. Soc.* **51**, 669–690.

Vladimirov, N. P. and Dmitriev, V. I.: 1972, 'Geoelectrical Section of the Earth Crust and Upper Mantle at East-European Platform in Accordance with MTS Data (in Russian)', *Izv. Akad. Nauk SSSR Fiz. Zemli* **6**, 100–103.

Velikhov, E. P., Dreizin, U. A., and Shamraev, I. M.: 1983, 'On Electromagnetic Sounding of Sedimentary Cover with Controlled Sources (in Russian)', *Doklady Akad. Nauk SSSR* **268**, 1090–1094.

Wannamaker, P. E., Hohmann, G. W., and SanFilipo, W. A.: 1984, 'Electromagnetic Modelling of Three-Dimensional Bodies in Layered Earths Using Integral Equations', *Geophysics* **49**, 60–74.

Wannamaker, P. E., Stodt, J. A., and Rijo, L.: 1986, 'Two-Dimensional Topographic Responses in Magnetotellurics Modeled Using Finite Elements', *Geophysics* **51**, 2131–2144.

Wannamaker, P. E., Booker, J. R., Jones, A. G., Chave, A. D., Filloux, J. H., Waff, H. S., and Law, L. K.: 1989, 'Resistivity Cross Section through the Juan de Fuca Subduction System and its Tectonic Implications', *J. Geophys. Res.* **94**, B10, 14.127–14.144.

Warner, B. N., Bloomguist, M. G., and Griffith, P. B.: 1983, 'Magnetotelluric Interpretation Based upon New Processing and Display Techniques', *53rd Ann. Internat. Mtg., Soc. Explor. Geophys.*, Expanded Abstracts, pp. 131–154.

Weidelt, P.: 1975, 'Electromagnetic Induction in Three-Dimensional Structures', *J. Geophys.* **41**, 85–109.

Wolfgram, P. and Scharberth, J.: 1986, *Electrical Conductivity Reference Exploration* (*ECRE*), Geometra Ltd., 18 pp.

Word, D. R., Goss, R. and Chamber, D. M.: 1986, 'An EMAP Case Study', *56th Ann. Internat. Mtg., Soc. Explor. Geophys.*, Expanded Abstracts, pp. 61–63.

Zhdanov, M. S. and Spichak, V. V.: 1980, 'Finite-Difference Modelling of Electromagnetic Fields over Three-Dimensional Geoelectrical Inhomogeneities (in Russian)', *Problemy Morskih Electromagnitnyh Issledovanij*, Moscow, IZMIRAN, pp. 102–114.

Zhdanov, M. S., Singer, B. Sh., Fainberg, E. B., Godneva, G. S., and Sanin, S. I.: 1987, 'Modelling of the Electromagnetic Fields in the Carpathian-Panonian Region (in Russian)', *Izv. Akad. Nauk SSSR Fiz. Zemli* **1**, 71–78.